

**An-Najah National University**

**Faculty of Graduate Studies**

**New Types of Dye-Sensitized Solar Cells Based  
on Natural Dyes**

**By**

**Malak Sabeeh Ahmed Saif**

**Supervisors**

**Prof. Hikmat S. Hilal**

**Dr. Ahed Zyoud**

**This Thesis is Submitted in Partial Fulfillment of the Requirements for  
the Degree of Master of Chemistry, Faculty of Graduate Studies, An-  
Najah National University, Nablus, Palestine.**

**2014**

Dedication

*To those who believed in me and taught me to strive for what I*

*believe in, gave me the strength when I was weak and always*

*been the shining stars in my life.*

*To my professors and placeable role models - my parents.*

*To my special gift from God - my husband.*

## **New Types of Dye-Sensitized Solar Cells Based on Natural Dyes**

*To all those who believe that with hard work come great*

*achievements.*

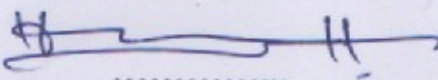
By

**Malak Sabeeh Ahmed Saif**

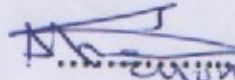
**This Thesis was defended successfully on 11 /12/2014 and approved by:**

### **Defense Committee Members**

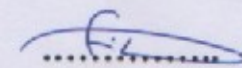
**1. Prof. Hikmat S.Hilal / Supervisor**

**Signature**  
  
.....

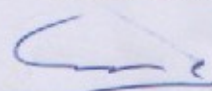
**2. Dr. Ahed Zyoud / Co-Supervisor**

  
.....

**3. Dr. Fuad Al-Rimawi / External Examiner**

  
.....

**4. Prof. Issam Abdelraziq / Internal Examiner**

  
.....

## **Detection**

*To those who believed in me and taught me to strive for what I believe in, gave me the strength when I was weak and always been the shining stars in my life.*

*To my precious irreplaceable role models ...my parents*

*To my special gift from God ...my husband*

*To my loving brothers, sister and sweet friends*

*To all those who believe that with hard work come great achievements*

*Malak Saif*

## **Acknowledgments**

I would like to express my deepest gratitude to my parents for all the believes they implanted in me and for all the sacrifices they made.

I have to thank my caring and supporting husband, my brothers and sisters for continued encouragement.

I also extend my gratitude to Professor Hikmat S. Hilal for honoring me with his supervision, thank you my doctor for all the patience, support and guidance through all my research period.

I am deeply indebted to my second supervisor Dr. Ahed Zyoud whose help, encouragement and suggestions motivated me to complete my work, thank you sir for being there whenever I needed you.

I would like to give special thanks to the laboratory technical staff in the Department of Chemistry and the Department of Physics at An-Najah National University.

I would like to express my every great appreciation to my doctors in the Chemistry Department at An-Najah National University; you have been such a role model to look up to.

Thanks are also extended to my grandparents for all the support, my friends and my colleagues at the chemistry department.

I would like to thank Al-Quds University staff for the AFM measurements.

## List of Contents

No.	Contents	page
	Detection	
	Acknowledgment	انا الموقع ادناه مقدم الرسالة التي تحمل عنوان :
	Declaration	
	List of tables	
	List of figures	
<b>New Types of Dye- Sensitized Solar Cells Based on Natural Dyes</b>		
<b>Chapter one: Introduction</b>		
1.1	Solar energy	
1.2	Solar cells	
1.3	Dye sensitized solar cells	
	Titanium dioxide thin films	
	Objectives	
1.5	Novelty	بحثي لدى اي مؤسسة تعليمية او بحثية اخرى.
<b>Chapter two: Experimental</b>		
2.1	Starting materials	
2.2	Equipments used	
2.3	Titanium dioxide thin film preparation	
2.3.1	Applying the titanium dioxide onto the FTO glass	
2.4	The solar cell construction	
2.5	Measurement technique	
2.6	Running the solar cell	
2.7	Solar cell stability measurement	
<b>Chapter three: Results and Discussion</b>		
3.1	Characterization results	
3.1.1	UV-vis characterization	
3.1.2	Solid film characterization	
3.1.2.1	Absorption spectra	
3.1.2.2	AFM characterization for titanium dioxide thin film electrodes	
3.2.1	AFM characterization for natural dye thin films	

Student's name:

اسم الطالب: ملاك مبريح أحم سيف

Signature:

التوقيع: ملاك مبريح أحم سيف

Date:

11/12/2014

التاريخ:

## List of Contents

No.	Contents	page
	<b>Detection</b>	iii
	<b>Acknowledgment</b>	iv
	<b>Declaration</b>	vi
	<b>List of tables</b>	ix
	<b>List of figures</b>	x
	<b>List of appreciations</b>	xiv
	<b>Abstract</b>	xv
	<b>Chapter one: Introduction</b>	1
1.1	Solar energy	2
1.2	Solar cells	3
1.3	Dye sensitized solar cells	4
1.4	Semiconductors	9
1.5	Titanium dioxide thin films	11
1.6	Hypothesis	15
1.7	Objectives	16
1.8	Novelty	16
	<b>Chapter two: Experimental</b>	17
2.1	Starting materials	18
2.2	Equipments used	18
2.3	Titanium dioxide thin film preparation	19
2.3.1	Cleaning FTO/glass substrates	19
2.3.2	Applying the titanium dioxide onto the FTO/ glass	19
2.3.3	Applying the natural dye onto the TiO <sub>2</sub> /FTO/glass	20
2.4	The solar cell construction	21
2.5	Characterization technique	23
2.6	Running the solar cell	23
2.7	Solar cell stability measurement	24
	<b>Chapter three: Results and Discussion</b>	25
3.1	Characterization results	28
3.1.1	Solution characterization	28
3.1.2	Solid film characterization	30
3.1.2.1	Absorption spectra	30
3.1.2.2	AFM characterization for titanium dioxide thin film electrodes	37
3.1.2.2.1	AFM characterization for anatase titanium dioxide thin films	37

<b>3.1.2.2.2</b>	AFM characterization for anatase titanium dioxide thin films	40
<b>3.2</b>	PEC results	43
<b>3.2.1</b>	Photo and dark J-V plots	44
<b>3.2.1.1</b>	Effect of type of natural dye	44
<b>3.2.1.2</b>	Effect of electrolyte	49
<b>3.2.1.3</b>	Effect of solution Ph	52
<b>3.2.1.4</b>	Effect of thickness of titanium dioxide layer	55
<b>3.2.1.5</b>	Effect of titanium dioxide crystal type	58
<b>3.3</b>	Stability measurement	60
	References	63
	المخلص	ب



## List of Tables

<b>No.</b>	<b>Table</b>	<b>Page</b>
<b>1.1</b>	Anatase and rutile titanium dioxide properties	14
<b>3.1</b>	PEC characteristics for naked and curcumin sensitized anatase titanium dioxide thin films	45
<b>3.2</b>	PEC characteristics for anthocyanin sensitized anatase titanium dioxide thin films	49
<b>3.3</b>	Effect of electrolyte type on PEC characteristics of anatase titanium dioxide thin films	50
<b>3.4</b>	Effect of electrolyte type on PEC characteristics of rutile titanium dioxide thin films	51
<b>3.5</b>	Effect of pH value of electrolyte on PEC characteristics of anatase titanium dioxide thin films	53
<b>3.6</b>	Effect of layer thickness on PEC characteristics of anatase titanium dioxide thin films	56
<b>3.7</b>	Effect of layer thickness on PEC characteristics of rutile titanium dioxide thin films	57
<b>3.8</b>	Effect of type of titanium dioxide on PEC characteristics of thin films	59

## List of Figures

No.	Figure	Page
<b>1.1</b>	Schematic view of dye sensitized solar cells	6
<b>1.2</b>	Curcumine chemical structure	8
<b>1.3</b>	Anthocyanin chemical structure	9
<b>1.4</b>	Position of the Fermi level in metals, semiconductors and insulators	10
<b>1.5</b>	Titanium dioxide crystal shape anatase, rutile and brookite	13
<b>2.1</b>	Schematic figure for Dr. blade technique	20
<b>2.2</b>	Atypical dye sensitized solar cell	22
<b>2.3</b>	Schematic diagram for PEC measurement	24
<b>3.1</b>	Reduction of copper ion in HCl electrolyte solution on glassy carbon electrode	28
<b>3.2</b>	Absorption spectra for extracted anthocyanin dye solutions, a) beets, b) red cabbage, c) roselle.	29
<b>3.3</b>	Absorption spectra for a) anthocyanin dye extracted from beets, b) curcumine dye	30
<b>3.4</b>	Absorption spectra for: a) anatase titanium dioxide solid thin film, b) rutile titanium dioxide solid thin film.	31
<b>3.5</b>	Absorption spectra for: a) anatase titanium dioxide solid thin film, b) anatase titanium dioxide thin film sensitized with curcumine.	32
<b>3.6</b>	Absorption spectra for anatase titanium dioxide thin film sensitized with anthocyanin extracted from a) roselle b) red cabbage c) beets.	33
<b>3.7</b>	Absorption spectra for: a) anatase titanium dioxide thin film sensitized with curcumine, b) anatase titanium dioxide sensitized with anthocynine extracted from roselle.	34
<b>3.8</b>	Absorption spectra for: a) rutile titanium dioxide thin film sensitized with anthocynine extracted from roselle, b) rutile titanium dioxide thin film sensitized with curcumine.	34
<b>3.9</b>	Absorption spectra for: a) rutile titanium dioxide thin film sensitized with anthocynine extracted from roselle, b) rutile titanium dioxide thin film sensitized with curcumine	35

<b>3.10</b>	Absorption spectra for: a) anatase titanium dioxide thin film sensitized with curcumine, b) rutile titanium dioxide thin film sensitized curcumine.	36
<b>3.11</b>	Absorption spectra for: a) rutile titanium dioxide thin film sensitized with anthocynine extracted from roselle b) anatase titanium dioxide thin film sensitized with anthocynine extracted from roselle.	36
<b>3.12</b>	Topography for a) naked anatase titanium dioxide thin film, b) anatase titanium dioxide thin film sensitized with curcumin	37
<b>3.13</b>	AFM images for a) naked anatase titanium dioxide thin film, b) anatase titanium dioxide thin film sensitized with curcumin	38
<b>3.14</b>	Average surface roughness analysis for a) naked anatase titanium dioxide thin film, b) anatase titanium dioxide thin film sensitized with curcumin	39
<b>3.15</b>	Surface depth profiling for a) naked anatase titanium dioxide thin film, b) anatase titanium dioxide thin film sensitized with curcumin	40
<b>3.16</b>	Topography for a) naked rutile titanium dioxide thin film, b) rutile titanium dioxide thin film sensitized with curcumin	41
<b>3.17</b>	AFM images for a) naked rutile titanium dioxide thin film, b) rutile titanium dioxide thin film sensitized with curcumin	41
<b>3.18</b>	Average surface roughness analysis for a) naked rutile titanium dioxide thin film, b) rutile titanium dioxide thin film sensitized with curcumin	42
<b>3.19</b>	Surface depth profiling for a) naked rutile titanium dioxide thin film, b) rutile titanium dioxide thin film sensitized with curcumin	43
<b>3.20</b>	Photo J-V plot for a) anatase titanium dioxide thin film sensitized with curcumin, b) anatase titanium dioxide thin film sensitized with anthocyanin extracted from roselle	45
<b>3.21</b>	Photo J-V plot for a) rutile titanium dioxide thin film sensitized with curcumin, b) rutile titanium dioxide thin film sensitized with anthocyanin extracted from roselle	46
<b>3.22</b>	Schematic structure for a) anthocyanin dye particle b) curcumin dye particle	47

<b>3.23</b>	Photo J-V plot for a) anatase titanium dioxide thin film sensitized with anthocyanin extracted from beets, b) anatase titanium dioxide thin film sensitized with anthocyanin extracted from red cabbage, c) anatase titanium dioxide thin film sensitized with anthocyanin extracted from roselle	48
<b>3.24</b>	Photo J-V plot for a) anatase titanium dioxide thin film sensitized with curcumin using iodine electrolyte, b) anatase titanium dioxide thin film sensitized with curcumin using sulfur electrolyte, c) anatase titanium dioxide thin film sensitized with curcumin using iron electrolyte	50
<b>3.25</b>	Photo J-V plot for a) rutile titanium dioxide thin film sensitized with curcumin using iodine electrolyte, b) rutile titanium dioxide thin film sensitized with curcumin using sulfur electrolyte, c) rutile titanium dioxide thin film sensitized with curcumin using iron electrolyte	51
<b>3.26</b>	Photo J-V plot for a) anatase titanium dioxide thin film sensitized with curcumin using basic iodine electrolyte, b) anatase titanium dioxide thin film sensitized with curcumin using acidic iodine electrolyte	52
<b>3.27</b>	dark J-V plot for a) anatase titanium dioxide thin film sensitized with curcumin using basic iodine electrolyte, b) anatase titanium dioxide thin film sensitized with curcumin using acidic iodine electrolyte	53
<b>3.28</b>	Photo J-V plot for a) rutile titanium dioxide thin film sensitized with curcumin using basic iodine electrolyte, b) rutile titanium dioxide thin film sensitized with curcumin using acidic iodine electrolyte	54
<b>3.29</b>	Dark J-V plot for a) rutile titanium dioxide thin film sensitized with curcumin using basic iodine electrolyte, b) rutile titanium dioxide thin film sensitized with curcumin using acidic iodine electrolyte	55
<b>3.30</b>	Photo J-V plot for a) anatase titanium dioxide thin film with a 150 $\mu\text{m}$ thickness, b) anatase titanium dioxide thin film with a 130 $\mu\text{m}$ thickness	56

<b>3.31</b>	Photo J-V plot for a) rutile titanium dioxide thin film with a 150 $\mu\text{m}$ thickness, b) rutile titanium dioxide thin film with a 130 $\mu\text{m}$ thickness	57
<b>3.32</b>	Photo J-V plot for a) anatase titanium dioxide thin film sensitized with curcumin, b) rutile titanium dioxide thin film sensitized with curcumin	58
<b>3.33</b>	Dark J-V plot for a) anatase titanium dioxide thin film sensitized with curcumin, b) rutile titanium dioxide thin film sensitized with curcumin	59
<b>3.34</b>	Short circuit current density vs. time measurement for anatase titanium dioxide thin film electrodes sensitized with curcumin	60

## List of Abbreviations and Definitions

<i>Symbol</i>	<i>Abbreviation</i>	<i>Definitions</i>
<b>AFM</b>	Atomic force microscopy	
<i>UV</i>	<i>Ultra violet</i>	
$E_g$	<i>Band Gap</i>	<i>Forbidden energy region between Valence Band and Conduction Band</i>
$E_F$	<i>Fermi Level</i>	<i>Hypothetical energy level at which the probability of finding the electron is 1/2.</i>
$\text{\AA}$	<i>Angstrom</i>	
$e^-$	<i>Electron</i>	
$h^+$	<i>Hole</i>	<i>Positive charge resulting from loss of electron by excitation</i>
<b>VB</b>	<i>Valance Band</i>	<i>Highest filled energy band in the crystal</i>
<b>CB</b>	<i>Conduction Band</i>	<i>Lowest empty energy band in the crystal</i>
$V_{oc}$	Open circuit voltage	The applied potential at which current does not occur
	Dark Current	Current that occurs in the dark with applied potential when the bands are falt
$I_{sc}$	Short circuit current	Current that occurs at zero applied potential, normally due to photo-excitation
$J_{sc}$	Short circuit current density	Short circuit current passing across a unit area of the semiconductor electrode
$\square$	Efficiency	Observed electric power resulting from 100 units of radiation power
<b>FF%</b>	Fill Factor	Ratio between maximum observed efficiency divided by maximum possible efficiency
<b>PEC</b>	Photo-electrochemical cell	

**New Types of Dye-Sensitized Solar Cells Based on Natural Dyes.****By****Malak Sabeeh Ahmad Saif****Supervisors****Prof. Hikmat S. Hilal****Dr. Ahed Zyoud****Abstract**

A new type of dye sensitized solar cells was constructed, many different parameters were investigated to enhance their efficiencies. Two types of titanium dioxide powders were used to prepare the TiO<sub>2</sub> thin film electrode for the cell. Anatase and rutile titanium dioxide thin film electrodes were prepared by the Dr. Blade technique. Anatase thin films were proved to give better results than rutile films under similar conditions, with a conversion efficiency of 0.22% and a fill factor of ~ 60%.

The solar cells were sensitized using two natural dyes, curcumine and anthocyanin (which was extracted from three sources; red cabbage, beets and roselle). Curcumine sensitized solar cells gave better conversion efficiencies than all three types of anthocyanins.

The PEC measurements were performed using three different types of electrolyte solutions: Iron, sulfur and iodine. Iodine electrolyte gave the best results for both solar cells sensitized with anthocyanin and with solar cells sensitized with curcumine. The effect of changing the pH value of the iodine electrolyte solution was also investigated; higher conversion efficiency was obtained using basic electrolyte solution.

The effect of TiO<sub>2</sub> layer thickness on PEC characteristics was also studied (130 μm and 150 μm). The 150 μm thin films gave better results for both anatase and rutile electrodes.



# **CHAPTER 1**

## **Introduction**

## **Introduction**

In our modern life-style, which is basically based on power, electrical devices and high technology, energy is becoming an essential need. With the growing world population, which is expected to reach 10 billion in 2050, more energy will be needed to fulfill the living standards [1].

Although most of the world's energy comes from fossil fuel, attention nowadays is being more directed towards finding new reliable and sustainable sources. That is basically because, not only fossil fuels have dangerous impacts on the environment, but they are also running out.

Renewable energy supplies, involving solar energy provide a satisfying energy source which is available, free and environmentally friendly sources [2].

### **1.1. Solar energy:**

The sunlight that reaches the earth surface every day exceeds the annual energy demand. Even though solar energy has some limitations, it still provides the most promising alternative source with very wide applications and so many advantages [1, 3, 4].

Solar energy provides:

1- An abundant source so we never have to worry about the energy source depletion.

2- A clean source with no emissions or massive severe effects on the environment.

3- Doesn't need complicated distribution networks since it directly reaches our homes.

Despite the great advantages of solar energy, it still has a number of shortcomings, such as:

- High cost of the initial equipment used to harvest the energy.
- It is affected by the weather and functions only in day light.
- It needs large area for sunlight installation [1].

## **1.2. Solar cells:**

The conversion of solar energy into useful energy comes through solar cells which convert the sunlight directly into electricity. Solar cells can be classified into two classes:

- Photovoltaic (PV) cells:

Modern solar photovoltaic cells are basically based on semiconductors which use the sunlight to initiate a photo-induced electron transfer reaction. The absorption of the sunlight photons causes an electron transfer from the valence band to the conduction band of the semiconductor. The excited electron can be used to drive a chemical reaction [5-7].

- Photo-electrochemical (PEC) cells:

Observations showed that voltage could be produced by placing two special electrodes in a redox electrolyte and irradiating the system with light. As the light photons hit the working electrode some electrons escape leaving behind a hole. Holes and electrons move in opposite directions, a current is generated that can drive a load. In this type of solar cells, a semiconductor/ electrolyte junction is used as the working electrode which releases electrons as the semiconductor absorbs the sunlight photons [4]. In these solar cells the semiconductor does both jobs of light absorption and charge transfer.

### **1.3. Dye sensitized solar cells (DSSC's):**

Dye sensitized solar cells, or so called Gratzel cells, were first reported in 1991. Since then they had attracted considerable attention from researchers to study the working principle and to find methods for increasing their conversion efficiency (Observed electric power resulting from 100 units of radiation power). Dye sensitized solar cells have many advantages, such as: low cost and effectiveness, easy and simple to manufacture, flexible and transparent [8] , not sensitive to the semiconductor defects and direct transfer from photons to chemical energy.

Although there are some efficiency problems facing DSSC's, they are still considered a very important type of solar cells. Dye sensitized solar cells are different from other semiconductor devices in which light absorption and charge transfer are separated. The sensitizer that is fixed on the surface

of a wide gap semiconductor plays an essential role in absorbing sunlight [9-11].

DSSC's are basically composed of a photoactive working electrode which is basically the wide gap semiconductor and a sensitizer, together with a counter electrode and a suitable redox couple (electrolyte), Figure (1.1).

These types of solar cells provide a rich field for research, in which there are many different aspects for studying and modifying such as: the type of the semiconductor materials, effect of different types of electrolytes, and stability of the devices [12].

Dyes are used as sensitizers that absorb the sunlight and then get oxidized as a result of an electron transfer from the sensitizer excited molecular orbital to the conduction band of the semiconductor. Another advantage for using dyes as sensitizers is that they help lower electron-hole recombination [12].

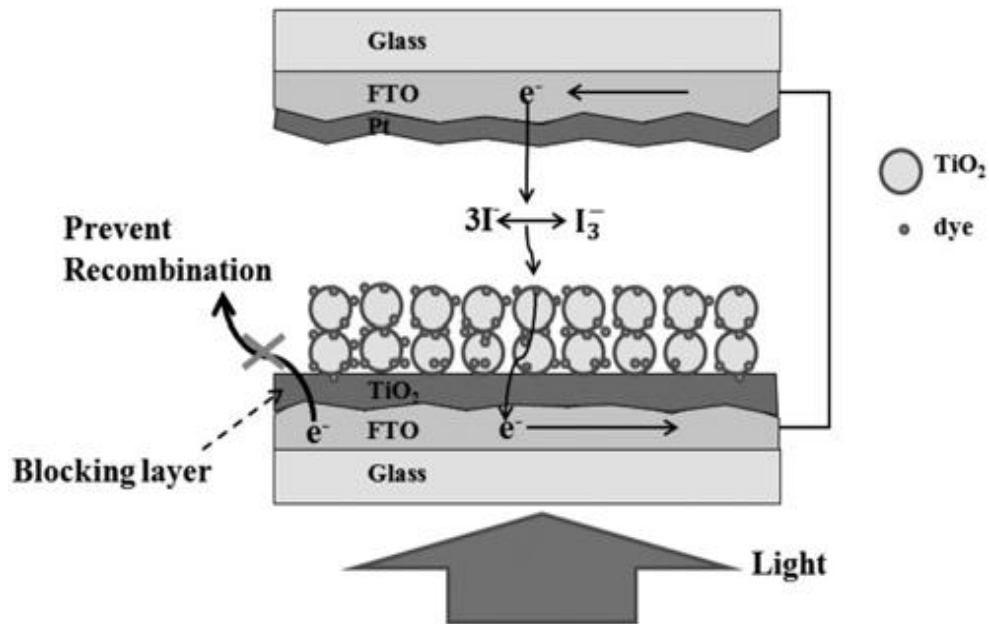


**Figure (1.1):** Schematic view of dye sensitized solar cells [13].

When DSSCs were first reported ruthenium complexes were used as sensitizers. Since then, the efficiencies of many compounds as photosensitizers have been studied such as: Porphyrins [14], phthalocyanines, coumarin 343 [15], carboxylated derivatives of anthracene and transition metal complexes [  $Ru(bpy)_3^{3+}$  ]. The  $d^6$  ruthenium polypyridyl complexes gave good results, due to the intense metal to ligand charge transfer bands in the visible region caused by the  $d^6$  metal complexes [12]. The high cost, long-term unavailability and heavy metal ruthenium sensitizers directed the attention towards finding new available, low cost sensitizers as alternatives.

Natural dyes are considered the best alternative as sensitizers for DSSC's due to their advantages, such as:

- 1- High molar extinction coefficient.
- 2- Available.
- 3- Easy to prepare.
- 4- Nontoxic.
- 5- Cheap.
- 6- Environmentally-friendly.
- 7- Narrow band gap.

Natural dyes with their narrow band gap values (absorb in the visible region) enhance the semiconductor efficiency, and broaden the photo action spectrum towards lower photon energy [11, 13, 16-22]. Numerous kinds of natural dyes extracted from leaves, flowers or roots are used as sensitizers for solar cells and gave acceptable conversion efficiencies [23, 24]. For example: Red Sicilian orange juice sensitized solar cells showed conversion efficiencies of 0.66% [23], sumac DSSCs showed 1.5% conversion efficiencies [23], dye sensitized solar cells using China rose as sensitizer produced a conversion efficiency of 0.27 %, and coffee sensitized solar cells gave conversion efficiency of 0.33 % [18].

Curcumine (bis (4-hydroxy-3-methoxyphenyl)-1, 6-heptadiene) as shown below in Figure (1.2), is a natural yellow-orange dye extracted from *Curcuma Longa* plant. The dye was used for many years for medical and food purposes. Curcumine has antioxidant and antibacterial effects. This safe available and easily prepared dye absorbs in the visible region 420-580 nm which makes it a very suitable sensitizer for DSSCs [20, 25, 26].

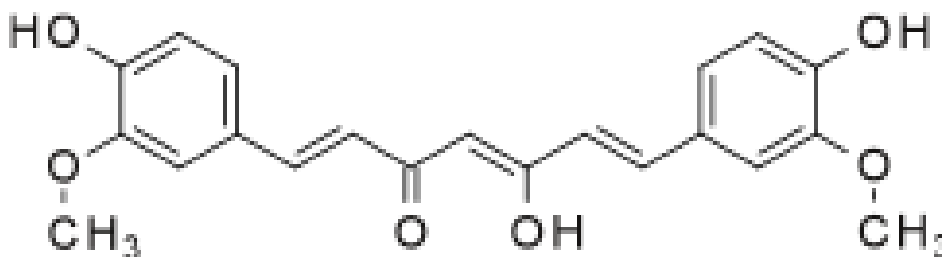


**Figure (1.2):** Curcumin chemical structure [27].

Curcumin dye sensitized solar cells which have not been widely studied and reported, showed conversion efficiency of 0.6% [20]. Furthermore, a structural modification of curcumin enhanced its sensitizing ability and reached a conversion efficiency of 7.6 % [28, 29].

Anthocyanins are water soluble natural pigments that are present in many kinds of plants, such as: Strawberry, grapes, beets, red cabbage and roselle ... etc. They are responsible for the red, blue and purple colors of the plant leaves, fruits or flowers. Anthocyanins are considered powerful antioxidants. The colors of Anthocyanins are affected by several factors such as: The concentration, the pH value, the chemical structure of the dye and the storage time [30, 31].

Anthocyanins are unstable towards light. They absorb in the uv-visible range. They are also unstable for pH changes as their color changes with different pH values. They degrade at high pH values. Therefore they are considered good pH indicators [32, 33].



Anthocyanins are glycosylated, polyhydroxy, and polymethoxy derivatives of 2-phenyl benzopyrylium salts. Figure (1.3) shows the general structure of Anthocyanins.

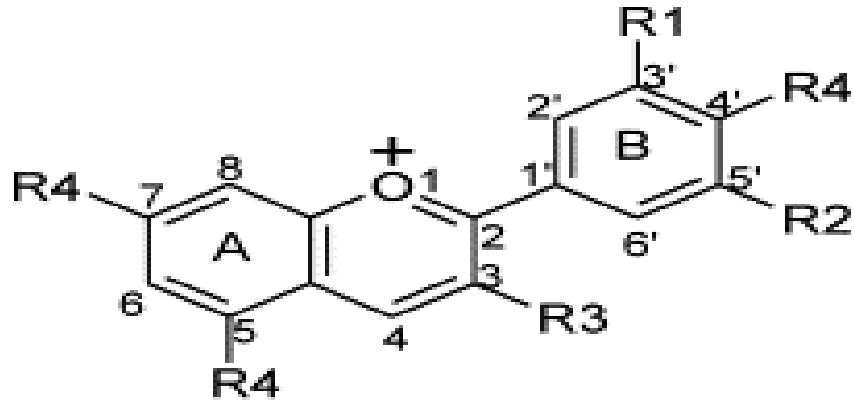
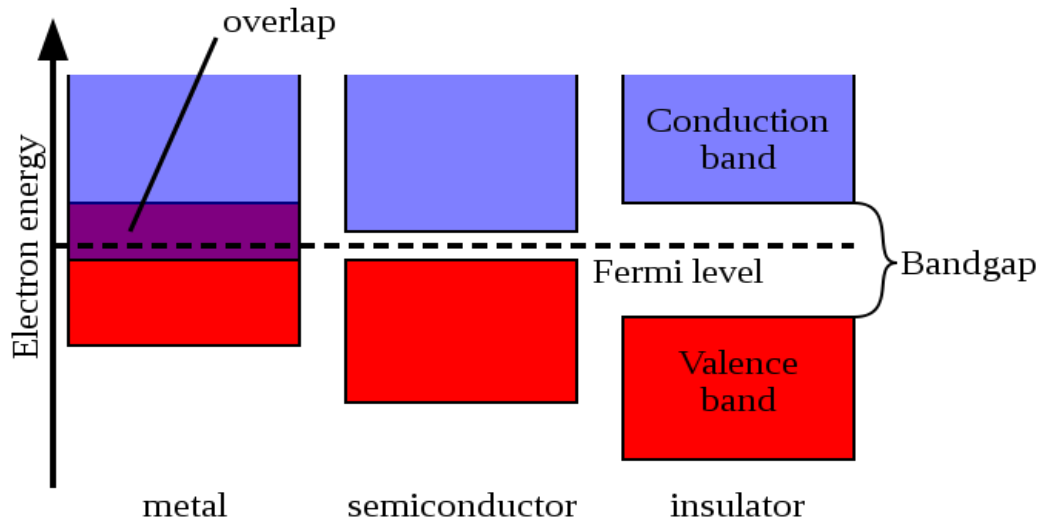


Figure (1.3): Chemical structure for Anthocyanin dyes [34].

#### 1.4. Semiconductors:

In a semiconductor the highest occupied molecular levels (HOMO) and the lowest unoccupied molecular levels (LUMO) are separated into two bands; the valance band and the conduction band with the Fermi level half way between them, as shown in Figure (1.4).



**Figure (1.4):** Position of the Fermi level in a) metal b) semiconductor c) insulator.

The Fermi level (*Hypothetical energy level at which the probability of finding the electron is 1/2*) is defined as the electrochemical potential of electrons in a material. The Fermi-Dirac distribution function states that at  $T = 0$  K all levels below the Fermi level are occupied with paired electrons, and at  $T > 0$  K some levels above the Fermi level are also occupied. Understanding the Fermi level is important to understand the properties of the material [1].

When a semiconductor absorbs a photon an electron is transferred from the valence band to the conduction band. This generates charge carriers inside the semiconductor. For the electron to be excited, the absorbed photon must have energy equal to or higher than the semiconductor band gap. The sunlight (with little UV) doesn't have enough energy to excite electron in the wide band gap semiconductors; which is the main drawback for wide band gap based devices [1, 5, 6]. Wide band gap semiconductors demand

high energy photons in the UV region. One common example of wide band gap semiconductors is titanium dioxide.

### **1.5. Titanium dioxide semiconductors:**

Both zinc oxide and titanium dioxide were used in the preparation of dye sensitized solar cells. Although both have many structural similarities they work differently in DSSC's. Titanium dioxide based solar cells showed better results than solar cells based on zinc oxide solar cells. This is attributed to lower electron injection efficiencies of the excited dye particles and lower dye regeneration effectiveness. Titanium dioxide is a wide band gap semiconductor with a 3.2 eV band gap that prevents the absorption in the visible region [35, 36]. Titanium dioxide semiconductors are widely used in dye sensitized solar cells, with a 11% conversion efficiency obtained when using ruthenium complexes as sensitizers [18, 37].

The metal complexes external ligands can easily bind to the surface of titanium dioxide, since the  $\text{TiO}_2$  surfaces with OH groups provide suitable sites for complexation. If the ligands were organic the complexation is considered a Lewis acid /Lewis base reaction in which the titanium dioxide surface acts as a Lewis acid and the ligands act as Lewis bases [38].

Titanium dioxide is known to have many physical and chemical properties that make it suitable. Examples of such properties are:

- Chemical Stability even at high temperatures [39].
- High dielectric constant. Materials with higher dielectric constant have much higher ability to store charge carriers in small area spaces than materials with low dielectric constant (which may suffer from charge leakage as the layer become thinner) [40].
- Photo-catalytic activity.
- Nontoxic material.
- High transmittance (transparent).

Nanocrystalline TiO<sub>2</sub> with suitable structure increases dye adsorption of the surface and facilitates the transport of electrons. The noticeable great performance of the semiconductor is due to the formation of interpenetrating hetero-junction bulk between the dye and the TiO<sub>2</sub> particles which are the electron transporting surface. The formation of a suitably thin, with a convenient structure, titanium dioxide layer on top of the conducting glass has a great importance [10, 12, 20].

Therefore many techniques have been used to prepare titanium dioxide thin films including:

- Electro-deposition.
- Dip-coating.
- Sol-gel.
- Chemical vapor deposition.
- Spin- coating.

- Dr. Blade technique.

All such techniques have been used in the fabrication of titanium dioxide electrodes for dye sensitized solar cells [8, 11, 13, 17, 41-48].

There are three main types of nanocrystalline titanium dioxide, namely anatase, brookite and rutile depending on the crystal structure, Figure (1.4). Production of these types depends on the preparation method and conditions [49]. Anatase (101) and rutile (110) are the most stable  $\text{TiO}_2$  crystal phases [38].

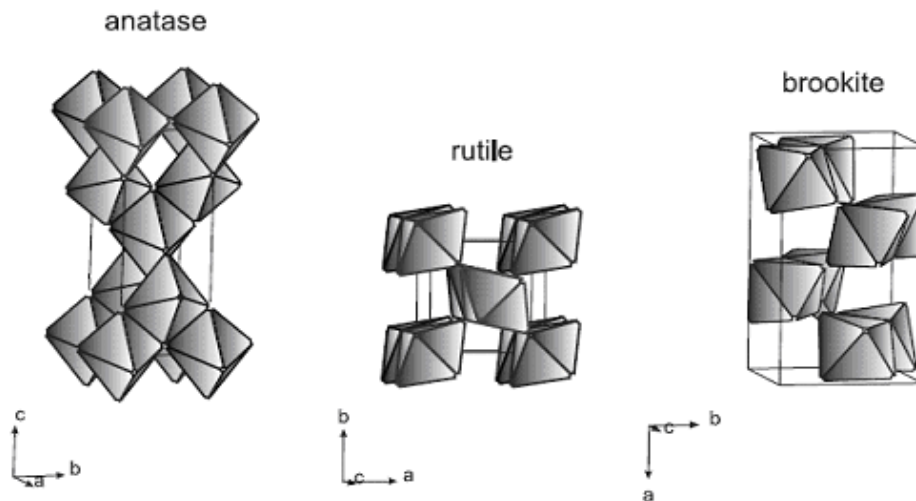


**Figure (1.5):** Titanium dioxide crystal shapes a) anatase b) rutile c) brookite [50].

These types have different properties mainly in their electronic properties. Some of their properties are listed in Table (1.1). Anatase has a 3.24 eV band gap and rutile has 3.02 eV [51].

**Table (1.1): Anatase and rutile titanium dioxide properties [50].**

<b>Properties</b>	<b>Rutile</b>	<b>Anatase</b>	<b>Brookite</b>
<b>Lattice constant a (Å)</b>	<b>4.59</b>	<b>3.78</b>	<b>9.18</b>
<b>Lattice constant b (Å)</b>	<b>4.59</b>	<b>3.78</b>	<b>5.45</b>
<b>Lattice constant c (Å)</b>	<b>2.95</b>	<b>9.52</b>	<b>5.15</b>
<b>Specific gravity</b>	<b>4.2 – 4.3</b>	<b>3.82 – 3.97</b>	<b>3.9 – 4.1</b>
<b>Index of refraction</b>	<b>2.74</b>	<b>2.52</b>	<b>2.58</b>
<b>Hardness (Mohs scale)</b>	<b>6.0 – 6.5</b>	<b>5.5 – 6.0</b>	<b>5.5 – 6.0</b>
<b>Melting point</b>	<b>1858 C°</b>	<b>1858 C°</b>	<b>1858 C°</b>

Anatase titanium dioxide properties include:

- Higher power density.
- Higher carrier mobility.
- Wider optical absorption gap.
- Smaller electron effective mass.
- Resistivity and Hall-effect results displayed an insulator-metal transition in a donor band in anatase with high donor concentration that was not present in rutile.

## 1.6. Hypothesis:

This work is basically "building up a curcumine sensitized Gratzel type solar cell, using two different types of titanium dioxide, and studying different parameters to improve its conversion efficiency".

The work is based on the following assumptions:

- Using heavy metal complexes as sensitizers in dye sensitized solar cells are not preferred.
- Metal ion complexes may be toxic and not easily available, so using natural dyes as an alternative is more convenient and less costly.
- Curcumine is a safe and available natural dye, which absorbs in the visible region.
- The type of the titanium dioxide used for the electrode preparation may affect the efficiency of the solar cell. In our work two types of titanium dioxide will be used anatase and rutile as they differ in their electronic properties and crystal shape. The effect of such differences on the efficiency of the solar cell will be studied.
- The type of the redox couple may also affect the solar cell activity.
- The acidity of the redox couple may affect conversion efficiency.
- The thickness of the titanium dioxide film may affect efficiency.

All such assumptions will be tested in this work.

### **1.7. Objective:**

Based on the above assumptions the main objective of our work will be to search for a new class of dye sensitized solar cells that are environmentally friendly, nontoxic, economic, highly efficient and stable. Curcumine will be used as a natural dye to sensitize two types of titanium dioxide film electrodes in a new Gratzel type solar cell.

### **1.8. Novelty:**

This work involves a number of novelty aspects, including:

- Studying the effect of the titanium dioxide type on a curcumine dye sensitized solar cell.
- Studying the effect of types of redox couple on curcumine dye sensitized solar cells efficiency.
- Studying the effect of acidity of the redox couple on the solar cell conversion efficiency.
- Studying the effect of the titanium dioxide layer thickness on the curcumine DSSC's conversion efficiency.

All such parameters will be studied here for the first time.



# **Chapter 2**

# **Experimental**

## **2.1. Starting materials:**

Common materials were purchased and used without further purification. Anatase and rutile titanium dioxide powders were purchased from Alfa Aesar.  $\text{FeCl}_3$ ,  $\text{Na}_2\text{S}$  and sulfur were purchased from Riedel. Ethanol and acetone from Aldrich.  $\text{FeCl}_2$ , HCl from Merck. Ethyl acetate, NaOH and KI purchased from Frutarom. High quality transparent FTO/glass substrates were purchased from Aldrich.

## **2.2. Equipment used:**

- The electronic absorption spectra for the extracted dye solutions and the  $\text{TiO}_2$  thin films were investigated using a Shimadzu (UV-3101 PC) UV-VIS-NIR- Scanning Spectrometer.
- The J-V measurements for the dye sensitized solar cells were done using a Computer controlled Princeton Applied research (PAR) model 263A Potential/ Galvanostate.
- Measuring the pH for the electrolyte solutions was done using a Jenway/3510 pH meter.
- Fluke 11 multimeter was used for measuring the dye sensitized solar cells resulting voltage.

## **2.3. Titanium dioxide thin film preparation:**

### **2.3.1. Cleaning FTO/glass substrates:**

All FTO/glass substrates were carefully cleaned before use, in order to obtain good adherence. The cleaning involved washing the substrates with soap and distilled water and then sonicating them for half hour with diluted HCl, finally sonicating for another half hour with acetone/ water solution. The substrates were kept in distilled water for further use.

### **2.3.2. Applying the titanium dioxide onto the FTO/glass:**

Titanium dioxide paste was prepared by mixing 3.0 g titanium dioxide powder with distilled water then adding (3-5) drops of acetic acid and mixing until we had a paste like structure. Titanium dioxide paste was applied to the FTO/glass substrates using the Dr. Blade technique as shown in Figure (2.1). The electrodes were dried for one hour on a hotplate.

To study the effect of the film thickness on the conversion efficiency of the prepared cells, the Dr. Blade was applied with tapes of different thicknesses placed on the edges of the FTO/glass, Titanium dioxide films with 130 and 150  $\mu\text{m}$  thicknesses were prepared.

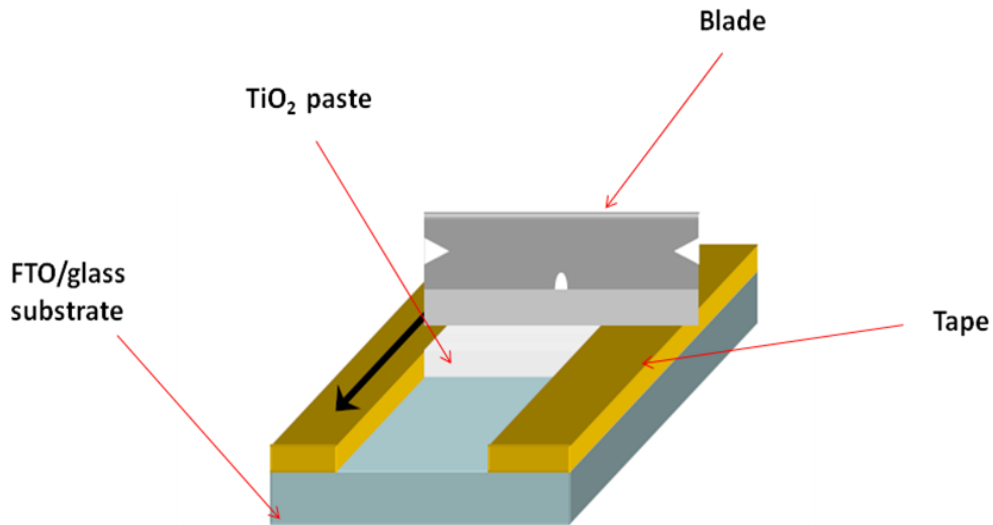


**Figure (2.1):** Schematic figure for Dr. Blade technique[52].

### **2.3.3. Extracting and applying the natural dye onto the TiO<sub>2</sub> /FTO/ glass:**

Two different types of natural dyes were used, anthocynine and curcumine. Anthocynine was extracted from red cabbage, beet and roselle by soaking 20.00 g of each in 100 ml ethanol with magnet-stirring on a plate for 1hr [53]. The dye solution was filtered and saved in the dark.

Curcumine was extracted from curcuma by mixing 20.00 g of curcuma in 100 mL ethyl acetate [54]. The mixture was stirred magnetically on a hotplate for 1 hr, then filtered and saved in the dark.

Anthocynine dye was applied onto the titanium dioxide thin film by soaking the film in the dye solution for 24 hrs. Curcumine was applied by adding 3-4 drops of the dye extract and letting to dry in the air. Curcumin

OH groups chemisorbed onto  $\text{TiO}_2$  surface easily leaving more permanent color.

#### **2.4. The solar cell construction:**

A typical dye sensitized solar cell was mainly composed of two electrodes: a working electrode (cathode) which was the titanium dioxide dye sensitized thin film, and a counter electrode (anode) which was a graphite coated FTO thin film. The anode was prepared by carbonating the FTO/ glass substrate using a candle until the color of the FTO/ glass substrate turned to black. The two electrodes were placed on top of each other after adding one drop of the electrolyte as shown in Figure (2.2).

Three different types of electrolyte solutions were prepared as follows:

- Iodine electrolyte was prepared by mixing  $\text{I}_{2(s)}$  (2.5g, 0.10M) with  $\text{KI}_{(s)}$  (1.6 g, 0.10M) with water (~50 mL) in a 100 mL volumetric flask and stirring until complete dissolution. The mixture was then diluted to the mark with distilled water, giving 0.10 M  $\text{I}_3^-$  final solution.
- Sulfur electrolyte was prepared by mixing  $\text{S}_{(s)}$  (0.32g, 0.10M),  $\text{NaOH}_{(s)}$ (0.399g,0.10M) and  $\text{Na}_2\text{S}_{(s)}$  (0.7798,0.10M) with water(~50 mL) in a 100 mL volumetric flask and stirring until complete dissolution.the mixture was then diluted to the mark with distilled water, giving  $\text{S}^{2-}$  (0.10 M)/S (0.10 M)/NaOH (0.10 M) final solution.
- Iron electrolyte was prepared by mixing  $\text{FeCl}_{2(s)}$  (1.3g, 0.10M) and  $\text{FeCl}_{3(s)}$  (1.6g, 0.01M) with water (~50 mL) in a 100 mL volumetric flask

and stirring until complete dissolution. The mixture was then diluted to the mark with distilled water, giving  $\text{Fe}^{+2}$  (0.10M) /  $\text{Fe}^{3+}$  (0.10M) system.

Few drops of sodium hydroxide solution were added to the iodine electrolyte until a pH equal to 11 was reached. The pH was measured by a Jenway/3510 pH-meter. The other two electrolytes were used without changing their pH, since changing the pH value may affect their nature. Lowering pH for sulfide solution converts it into  $\text{H}_2\text{S}$  gas, and increasing pH for Fe ions converts them into solid iron hydroxides. The sulfur electrolyte has a basic nature and the iron electrolyte has an acidic nature.

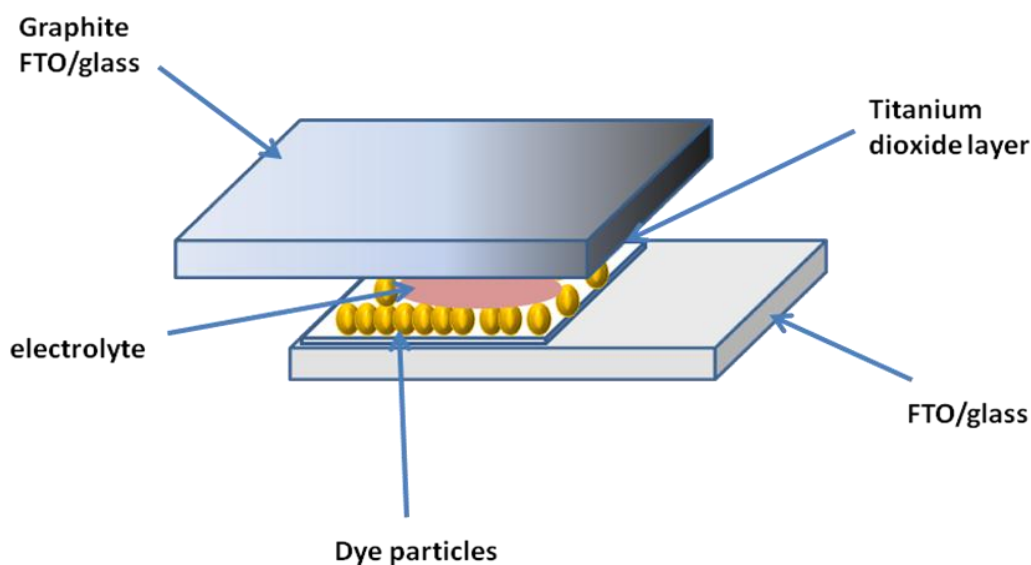


**Figure (2.2):** A typical dye sensitized solar cell.

## **2.5. Characterization techniques:**

### **- Solutions:**

The optical absorption spectra of the extracted dye solutions were studied at room temperature using a Shimadzu (UV-3101 PC) UV-VIS-NIR-Scanning Spectrometer in the wavelength range 400-800nm.

### **- Solid films:**

The UV- Visible absorption spectra of the prepared titanium dioxide electrodes were studied at room temperature in the wavelength range of 200-800 nm using UV-1601 Spectrometer.

## **2.6. Running the solar cell:**

The manufactured cell was connected to a Fluke 11 multimeter and exposed to a 50 Watt halogen spot lamp as a photon source. The voltage produced by the cell was measured.

To measure density vs. voltage (J-V) plots, the prepared dye sensitized solar cell was connected to a computer controlled Princeton Applied Research (PAR) model 263A Potential/ Galvanostat. For illumination a 50 Watt halogen spot lamp was used. The lamp has an intense coverage of wide spectral range between 450-800 nm with a high stability. Figure (2.3) describes the PEC connections. As shown in the figure no reference electrode was used in the measuring process. The counter electrode was connected to the cell photoanode, the working electrode was connected to

the cell photocathode. The light source was vertically directed towards the photocathode.

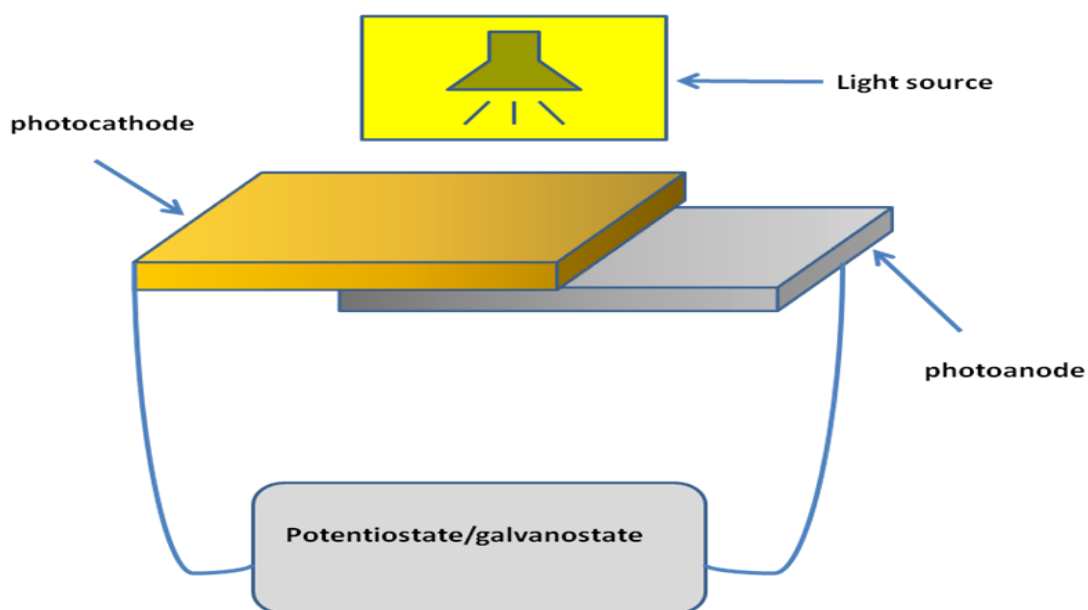


**Figure (2.3):** Schematic diagram for PEC measurement.

## 2.7. Solar cell stability measurement:

Polarographic analyzer (Pol 150) and polarographic stand (MDE 150) were used to study the solar cell stability under PEC conditions as described formerly. The values of short circuit current  $J_{SC}$  were measured vs. time. All measurement were done at room temperature using iodine electrolyte (0.01 M  $I_2$ , 0.01 M KI ).



# **Chapter 3**

## **Results and Discussion**

## Results and discussion

DSSCs drew a lot of attention since they were reported by M. Gratzel in the 1990s. The simple manufacturing process, low cost and acceptable work efficiency qualified them to be a competing future candidate.

DSSCs include many aspects such as: counter electrodes, sensitization techniques, electrolyte solutions and nanocrystalline layers. These areas provide a very rich field for research and development.

In our work we are focusing on investigating different parameters, for the sake of enhancing of TiO<sub>2</sub> based solar cells. We expect the crystal shape of the used TiO<sub>2</sub> to affect the cell efficiency since any structural defects may cause undesired electron recombination. As mentioned in Chapter one, two common types of titanium dioxide will be used in the thin film preparation.

Sensitizers play a key role in absorbing the sunlight, ruthenium complex were the first used sensitizers. Protoporphyrin-sensitized TiO<sub>2</sub> solar cell using Co(II / III) electrolyte reached a conversion efficiency of 12.3%, but the high cost and potential hazardous effects limited their use as photosensitizers. Since natural dyes provide a suitable choice, numerous kinds of dyes were studied and used as photosensitizers.

A screen study for anthocyanin sensitized solar cells was done, using anthocyanin from three locally available sources; red cabbage, beets and roselle. Curcumine sensitized solar cells were reported but not fully

investigated. Previous researches focused on the acidity degree of the dye. These two available and cheap natural dyes were used as photosensitizers in our work.

As mentioned above the type of electrolyte solution is with great importance. Different kinds of electrolyte solutions were reported and investigated. But the effect of the pH value of the electrolyte solution on the efficiency of the solar cell will be discussed for the first time.

In the hypothesis section we are also assumed that the layer thickness in the thin film preparation would have great effect on the solar cell.

All these parameters were studied and for a complete vision many techniques were used to characterize the prepared solar cells, electrode thin film and dye solutions, as presented in this Chapter.

For photocurrent measurements, a 50 Watt halogen spot lamp was used. For dark current measurements complete dark was obtained by using thick blanket cover. In both cases, the measurements were done at room temperature, using iodine, iron and sulfur electrolyte systems. The Potntiostat/Galvanostat had three electrodes. The working electrode was connected to SC electrode. The counter electrode was connected to the cell counter electrode. The reference electrode was also connected to the counter electrode of the cell, with internal reference used. The internal reference potential was calibrated vs. an AgCl/Ag reference, as shown in Figure (3.1).

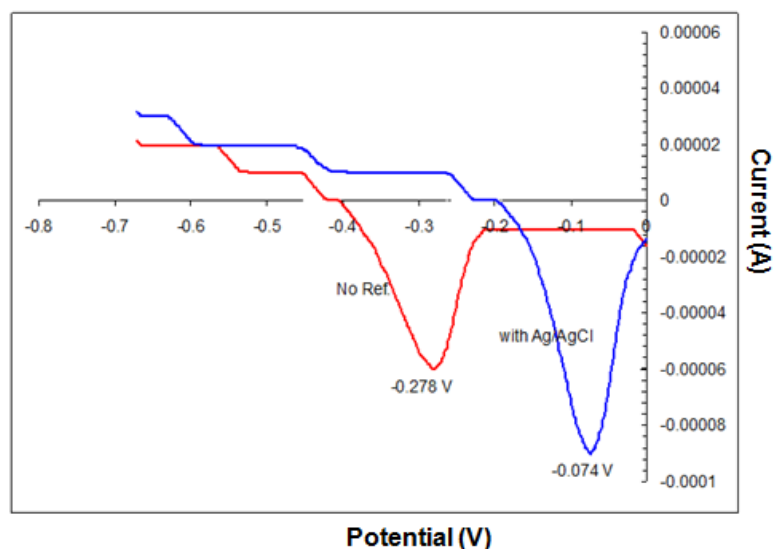


**Figure (3.1):** Potentiostat calibration results using reduction of copper ion in HCl electrolyte solution, on glassy carbon electrode.

From the Figure (3.1), the internal reference electrode showed 0.204 V more negative than AgCl/Ag reference. This means that the internal reference of the Potntiostat is equivalent to that of SHE. Thus all J-V plots measured in this work are shown with reference to SHE, unless otherwise stated.

### 3.1. Characterization results:

The electronic absorption spectra for the extracted dye solutions and for the titanium dioxide thin film electrodes were obtained as follows:

#### 3.1.1. Solution characterization:

The electronic absorption spectra for both curcumine and anthocynine dye solutions were studied at room temperature over a wavelength range

between 400-800 nm. The absorption spectra for the anthocynine solutions extracted from red cabbage, beets and roselle are shown in Figure (3.2).

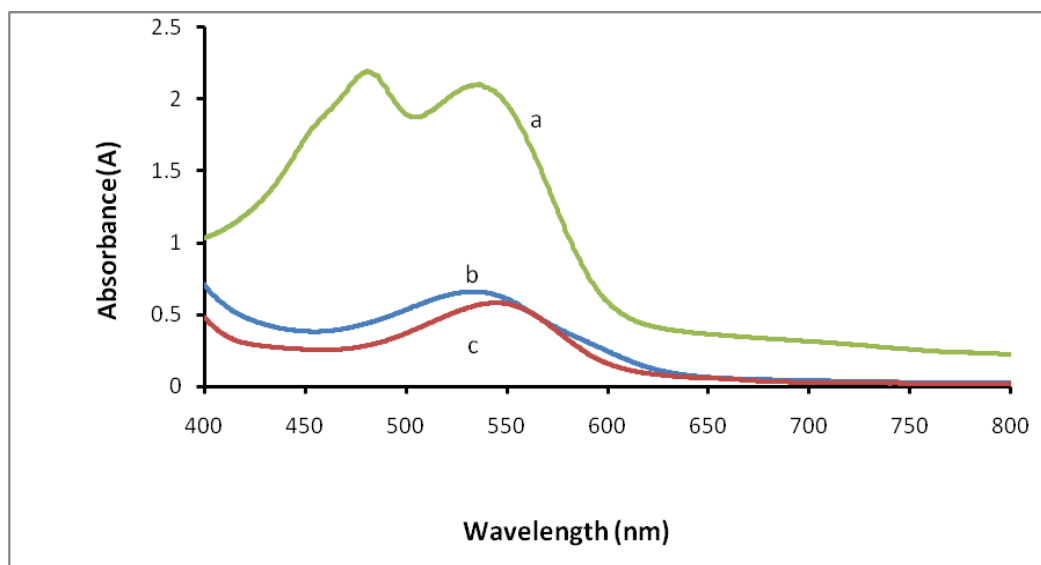


**Figure (3.2):** UV-VIS. Absorption spectra for anthocynine dye solutions extracted with ethanol from: a) beet b) cabbage c) roselle.

Anthocyanin extracted from roselle showed absorbance with  $\lambda_{\max} = 545$  nm , cabbage showed absorbance with  $\lambda_{\max} = 534$  nm while beets showed absorbance with two  $\lambda_{\max} = 480.5$  and  $535.5$  nm. The spectra prove that all three kinds of anthocyanin absorb near 500 nm which indicates a band gap value of about ( $\approx 2$  eV). This is consistent with earlier reports [20, 25-26].

The UV-VIS absorption spectra for curcumin dye Figure (3.3) shows that Curcumin exhibits a strong absorption band in the visible range due to its presence in the enol form. Enolization of curcumin allows  $\pi \rightarrow \pi^*$  transition that causes the absorption in the visible range and the appearance of the yellow color [20]. The spectra indicate that Curcumin dye absorbs

at shorter wave length (412 nm) and shows an intense absorption band over anthocyanin in the visible region.

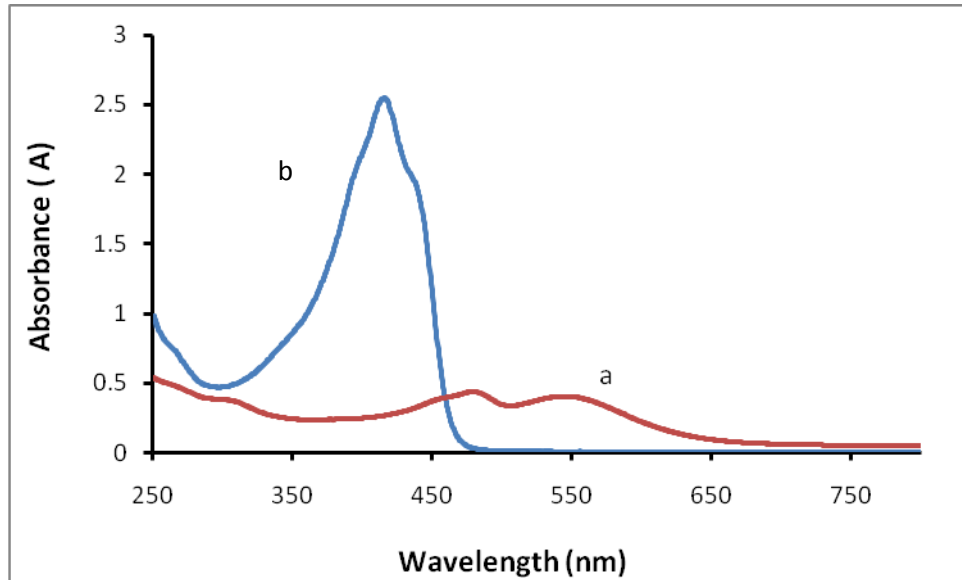


**Figure (3.3):** UV-VIS. Absorption spectra for a) anthocyanine dye extracted with ethanol from beets, b) curcumine dye extracted with ethyl acetate.

### 3.1.2. Solid film characterization:

The prepared titanium dioxide thin film electrodes were characterized, before sensitization with the dye solutions and after sensitization. Results are shown below.

#### 3.1.2.1. Absorption spectra:

The UV-visible absorption spectra were carried out at room temperature over a wavelength range 200-800 nm. Solid films of both anatase and rutile titanium dioxide were covered with curcumine dye particles and anthocyanine particles. Figure (3.4) shows the absorption spectra for anatase and rutile titanium dioxide without the dye particles on the surface.

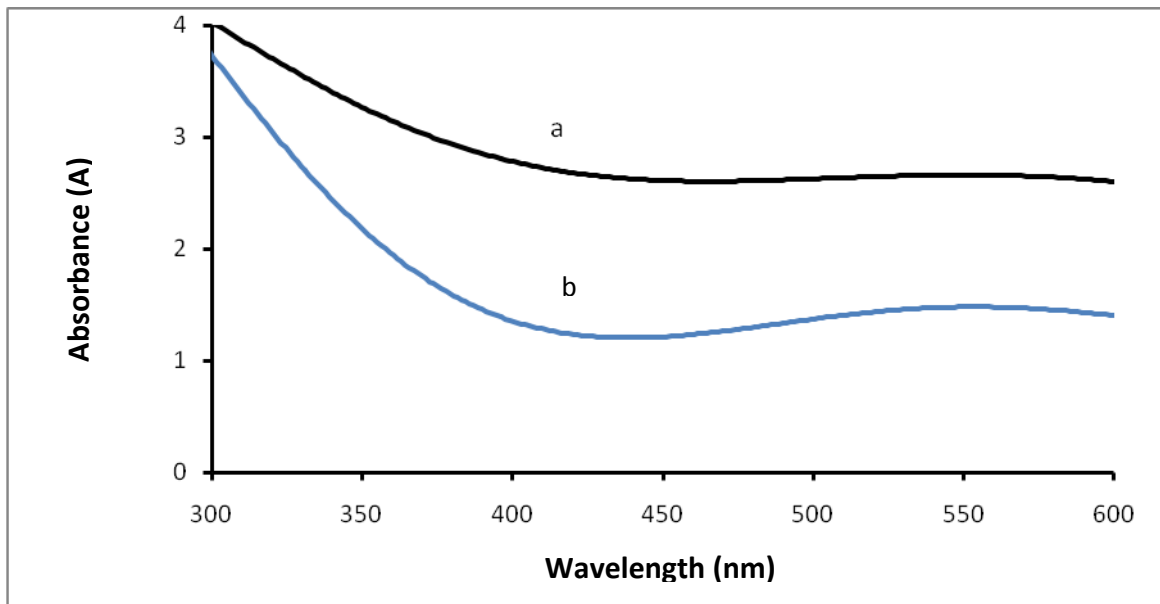


**Figure (3.4):** UV-VIS. Absorption spectra for: a) anatase titanium dioxide solid thin film, b) rutile titanium dioxide solid thin film.

The Figure (3.4) indicates that the anatase titanium dioxide thin film electrode showed an absorption edge of about 380 nm, with band gap of 3.2 eV. The absorption spectra for the rutile  $\text{TiO}_2$  Thin film showed an absorption edge of about 405 nm with 3.06 eV band gap.

Figure (3.5) shows the electronic absorption spectra for anatase titanium dioxide thin film and anatase titanium dioxide thin film sensitized with curcumine.

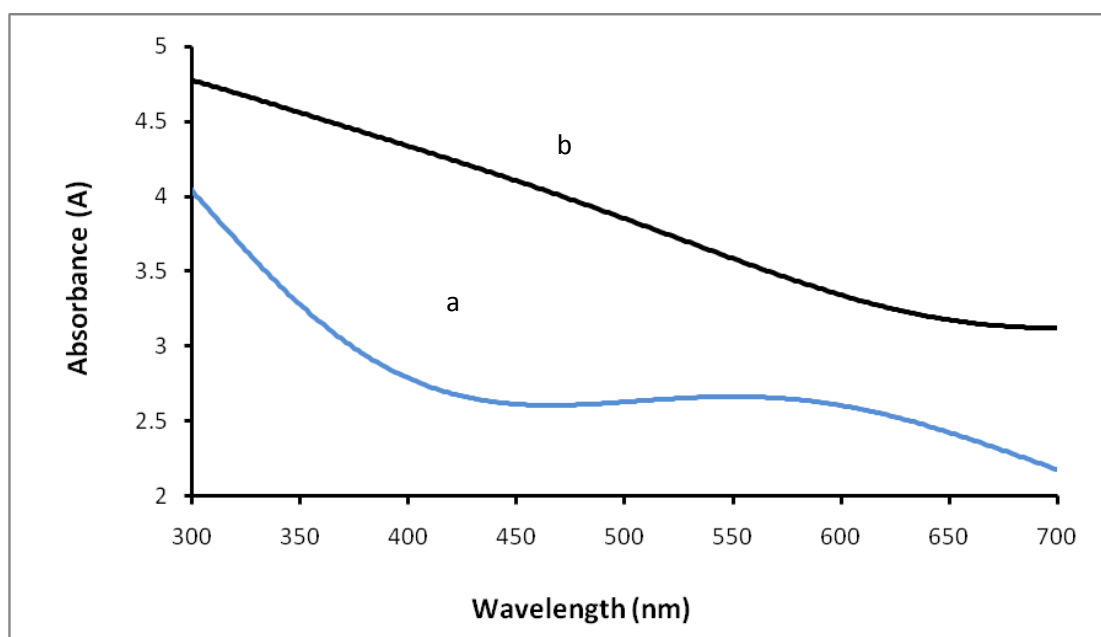
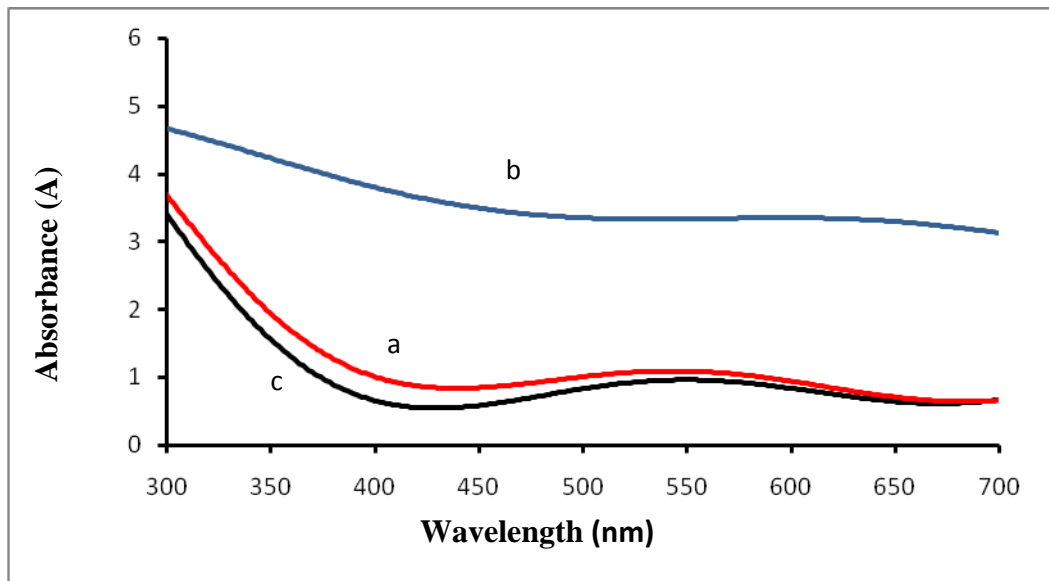


**Figure (3.5):** UV-VIS. Absorption spectra for: a) anatase titanium dioxide solid thin film, b) anatase titanium dioxide thin film sensitized with curcumine.

The curcumine sensitized thin film showed an absorption edge of about 630 nm with a band gap value of 1.97 eV, and also exhibited a stronger absorption over the other one. Curcumine dye absorbs in the visible region and adding it to the titanium dioxide layer broaden the absorption spectra and lowers the band gap value which enhances the photo – activity of the thin film.

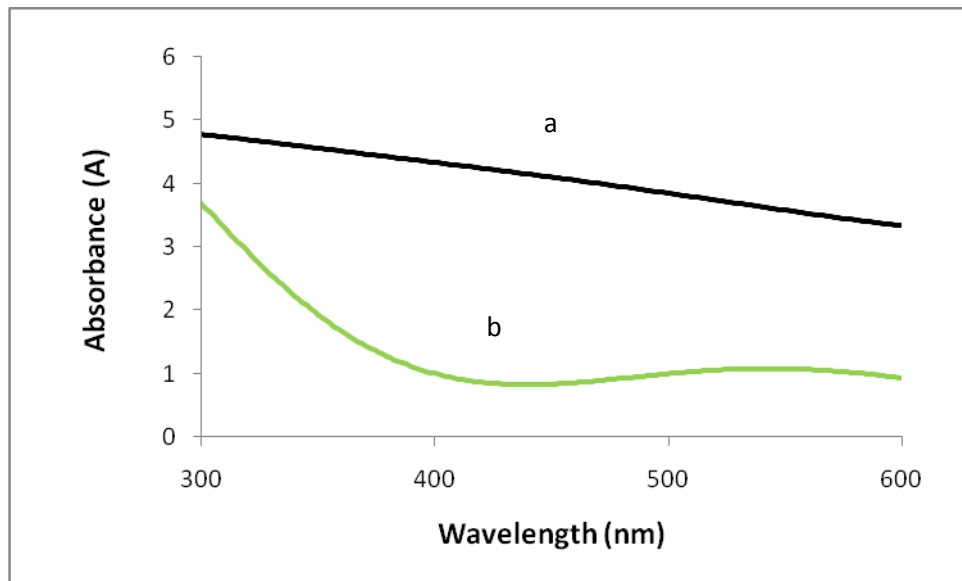
Anthocynine was extracted from three different sources, the electronic absorption spectra for anatase titanium dioxide thin film sensitized with anthocynine from the three sources was investigated Figure (3.6). The titanium dioxide thin film sensitized with anthocyanin extracted from roselle shows an absorption band at wave length shorter than the other two anthocyanin dyes.





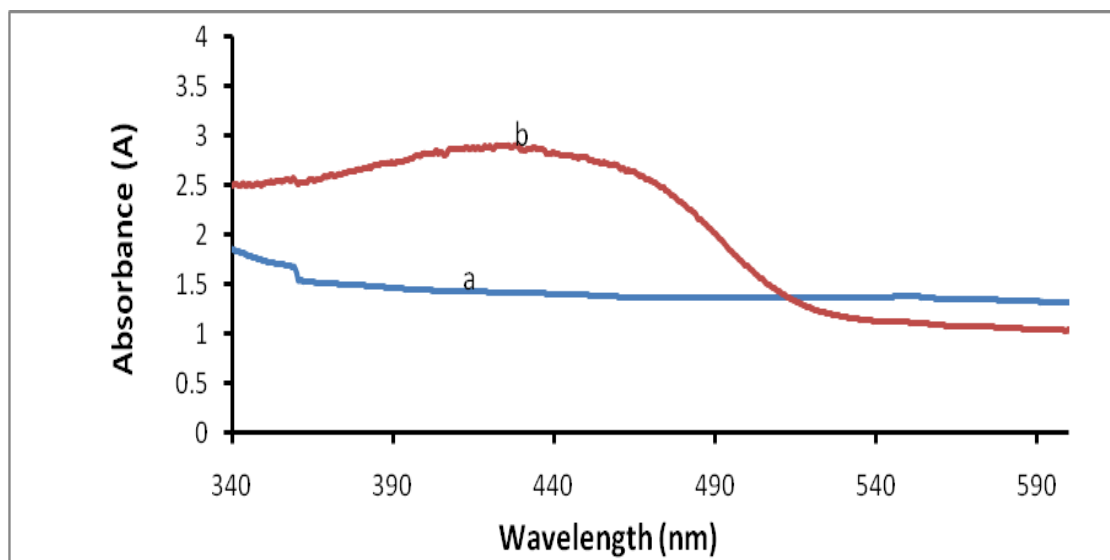
**Figurer (3.6):** UV-VIS. Absorption spectra for anatase titanium dioxide thin film sensitized with anthocyanin extracted from a) roselle b) red cabbage c) beets.

The absorption spectra for anatase titanium dioxide thin film sensitized with curcumine was compared with the anatase titanium dioxide thin film sensitized with anthocynine extracted from roselle, Figure (3.7). The changes in the spectra for both thin films indicate that the dye was absorbed on the thin film surface. Anatase titanium dioxide thin film sensitized with curcumine exhibits a much more enhanced absorption band in the visible region with an absorption edged of about 630 nm (band gab 1.96 eV), while anthocyanin sensitized thin film absorbs at shorter wave lengths with an absorption edge of about 445 nm (2.7 eV).



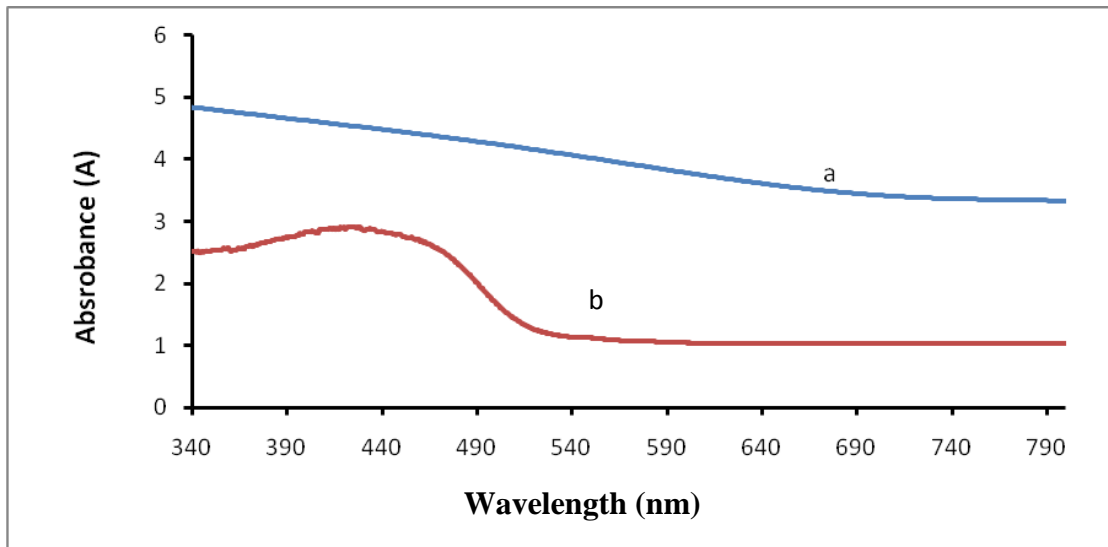
**Figure (3.7):** UV-VIS. Absorption spectra for: a) anatase titanium dioxide thin film sensitized with curcumine, b) anatase titanium dioxide sensitized with anthocynine extracted from roselle.

The same comparison was made for the rutile titanium dioxide thin films shown in the Figures (3.8) and (3.9) below. In Figure (3.8), the absorption spectra for rutile titanium dioxide sensitized with curcumine shows an absorption edge of about 510 nm with a band gab value of 2.43 eV.



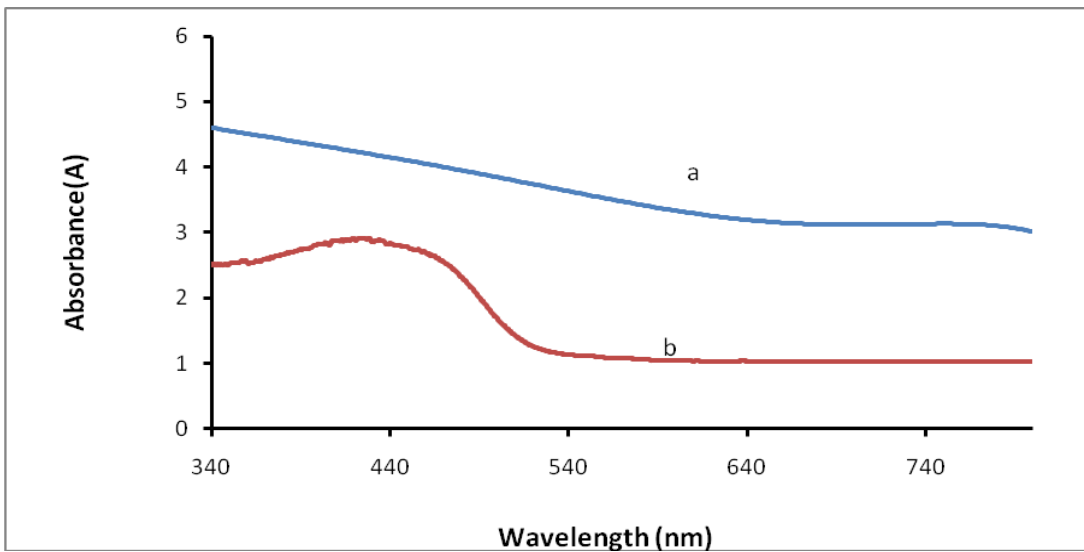
**Figure (3.8):** UV-VIS. Absorption spectra for: a) rutile titanium dioxide thin film b) rutile titanium dioxide thin film sensitized with curcumine.

Figure (3.9) shows the absorption spectra for rutile titanium dioxide thin film sensitized with curcumine and rutile titanium dioxide sensitized with anthocyanin extracted from roselle, curcumine sensitized thin film shows absorption spectra at shorter wavelength.



**Figure (3.9):** UV-VIS. Absorption spectra for: a) rutile titanium dioxide thin film sensitized with anthocyanine extracted from roselle, b) rutile titanium dioxide thin film sensitized with curcumine.

Anatase titanium dioxide thin films gave different results compared with rutile titanium dioxide thin films as observed from Figures (3.10) and (3.11). Figure (3.10) shows that anatase titanium dioxide thin film sensitized with curcumine exhibits a strong absorption starts at long wavelength values while rutile thin films absorbs at shorter wavelengths.



**Figure (3.10):** UV-VIS. Absorption spectra for: a) anatase titanium dioxide thin film sensitized with curcumin, b) rutile titanium dioxide thin film sensitized curcumin.

Figure (3.11) shows the absorption spectra for anatase and rutile titanium dioxide thin films both sensitized with anthocyanin, anatase titanium dioxide thin film also exhibits a strong absorption at longer wavelengths, while rutile absorbs at shorter wavelengths.

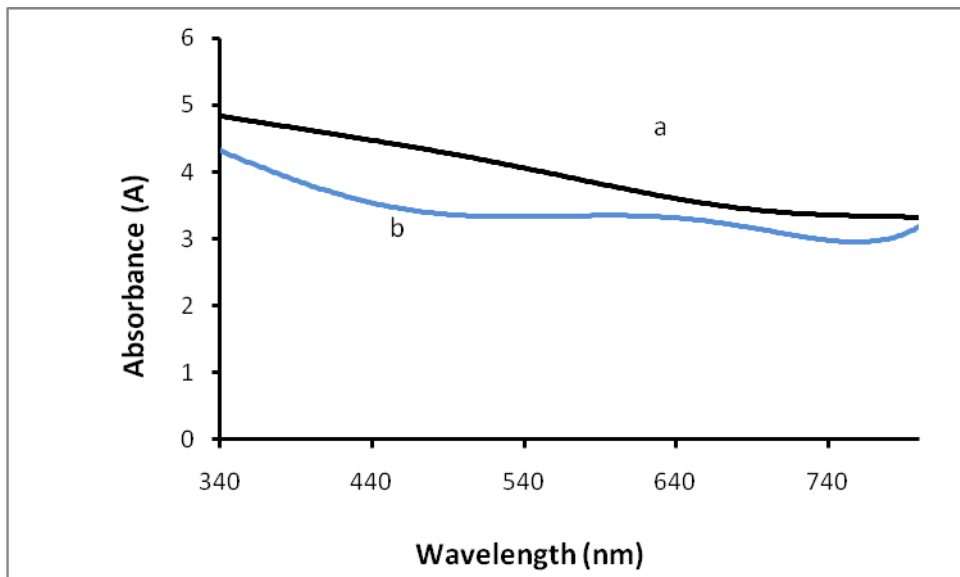


**Figure (3.11):** UV-VIS. Absorption spectra for: a) rutile titanium dioxide thin film sensitized with anthocyanine extracted from roselle b) anatase titanium dioxide thin film sensitized with anthocyanine extracted from roselle.

### 3.1.2.2 AFM characterization for titanium dioxide thin film electrodes:

AFM was used to study the surface morphology of the anatase and rutile titanium dioxide thin films. The 2D and 3D AFM images were obtained for the  $\text{TiO}_2$  thin films before sensitization and after sensitization with curcumin dye.

#### 3.1.2.2.1 AFM characterization for anatase $\text{TiO}_2$ thin films:

The topography for the naked anatase and curcumin sensitized titanium dioxide thin films is shown as 3D AFM images, Figure (3.12).

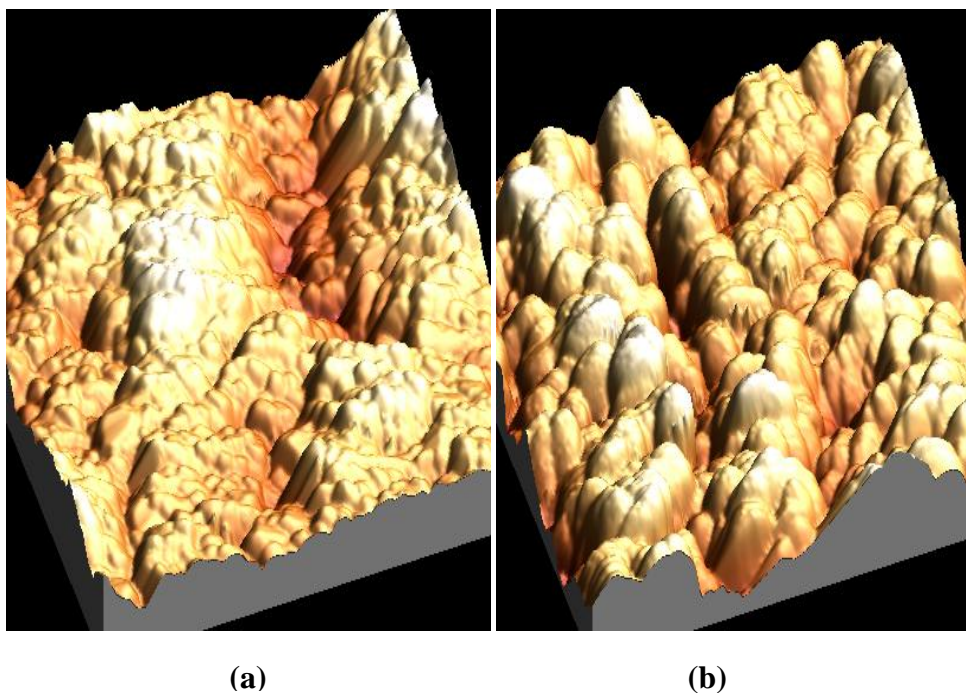


**Figure (3.12):** Topography for a) naked anatase titanium dioxide thin film, b) anatase titanium dioxide thin film sensitized with curcumin.

Both films showed holes and terraces. Films of anatase titanium dioxide sensitized with curcumin showed less holes with smoother grains than naked titanium dioxide film.

2D AFM images, Figure (3.13) (a), showed agglomerates of anatase TiO<sub>2</sub> nano-particles before sensitization with curcumin, Figure (3.13)(b), showed TiO<sub>2</sub> nanoparticles sensitized with curcumin. The Figure shows that films of anatase titanium dioxide sensitized with curcumin showed higher homogeneity, smoother surface and higher resolution than naked TiO<sub>2</sub> films.

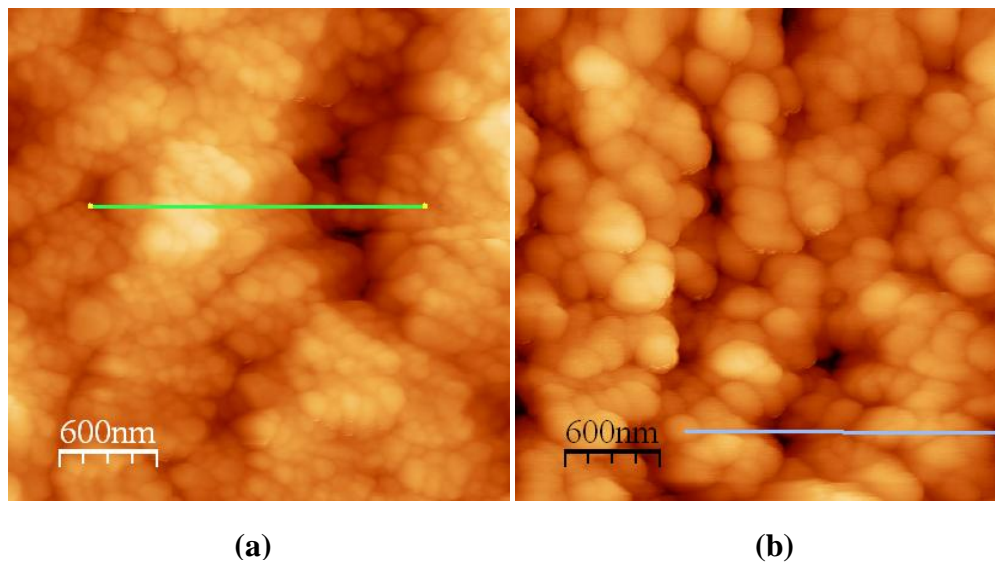


**Figure (3.13):** AFM images for a) naked anatase titanium dioxide thin film b) anatase titanium dioxide thin film sensitized with curcumin.

Values of root mean square (RMS) roughness were obtained from average surface roughness analysis, Figure (3.14).

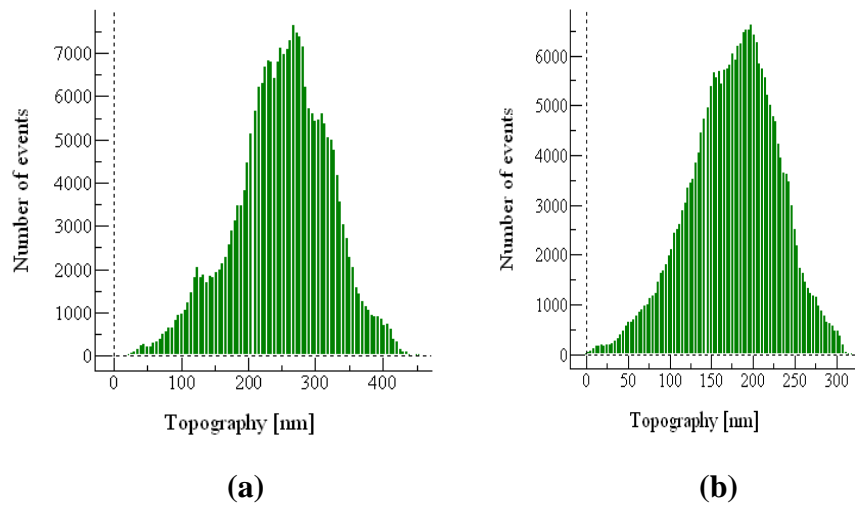


**Figure (3.14):** Average surface roughness analysis for a) naked anatase titanium dioxide thin film b) anatase titanium dioxide thin film sensitized with curcumin.

Figure (3.15) shows the surface depth profiling for naked and curcumin sensitized anatase titanium dioxide thin films. Both films showed holes and terraces distributed randomly at the surface. However, higher compactness clusters were obtained for the titanium dioxide films sensitized with curcumin.

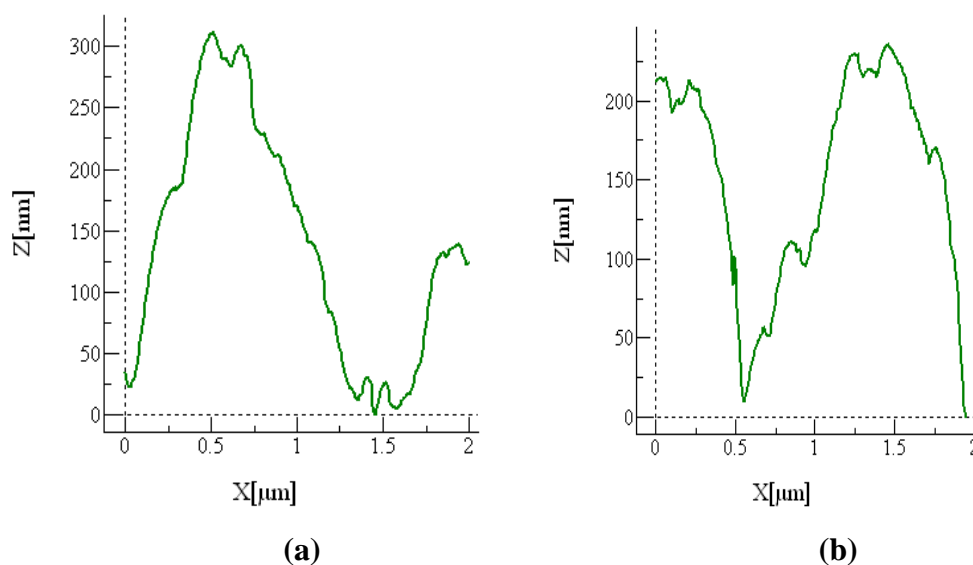


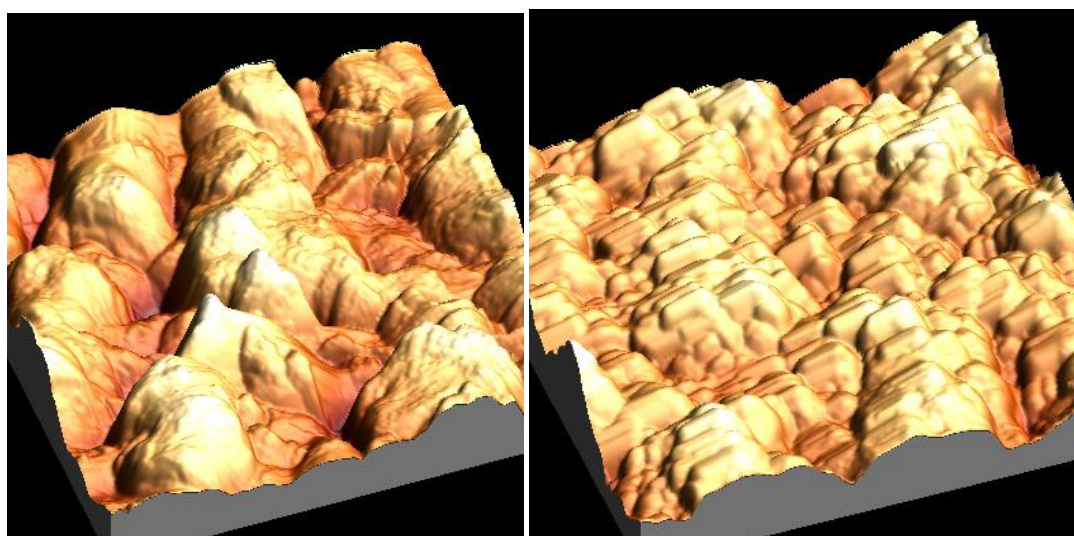
**Figure (3.15):** Surface depth profiling for a) anatase titanium dioxide thin film b) anatase titanium dioxide thin film sensitized with curcumin.

The AFM results finally indicate that the anatase  $\text{TiO}_2$  films (both naked and sensitized) well adhered onto the FTO/ glass surface.

### 3.1.2.2.2 AFM characterization for rutile $\text{TiO}_2$ thin films:

The topography for the naked and curcumin sensitized rutile titanium dioxide thin films is shown as 3D AFM images, Figure (3.16). Rutile titanium dioxide thin films sensitized with curcumin showed less holes and terraces than naked rutile titanium dioxide thin films.



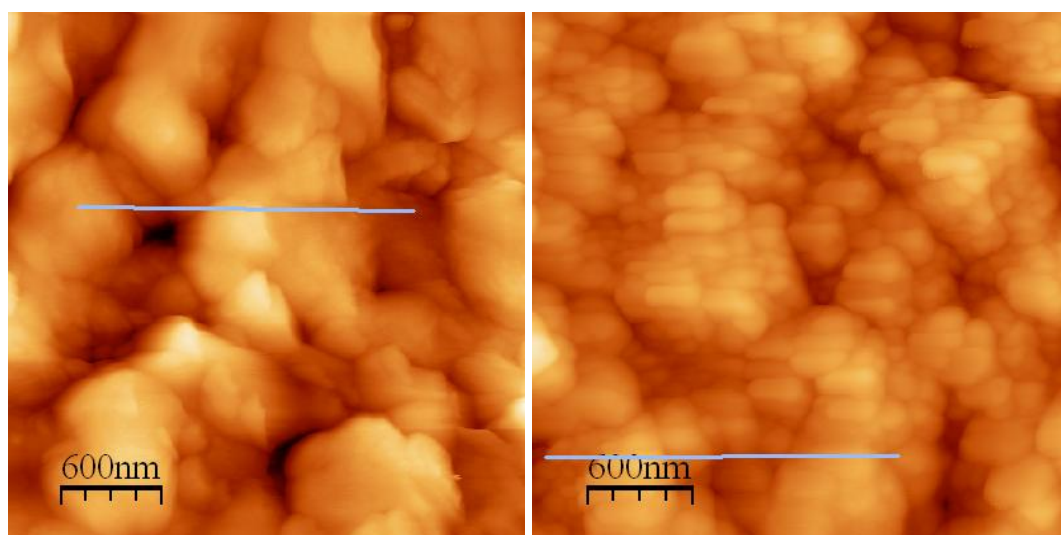


(a)

(b)

**Figure (3.16):** Topography for a) naked rutile titanium dioxide thin film, b) rutile titanium dioxide thin film sensitized with curcumin.

2D AFM images for rutile titanium dioxide thin films before and after sensitization with curcumin, are shown in Figure (3.17). Films of rutile  $\text{TiO}_2$  sensitized with curcumin showed higher homogeneity, and higher resolution than naked rutile titanium dioxide thin films.

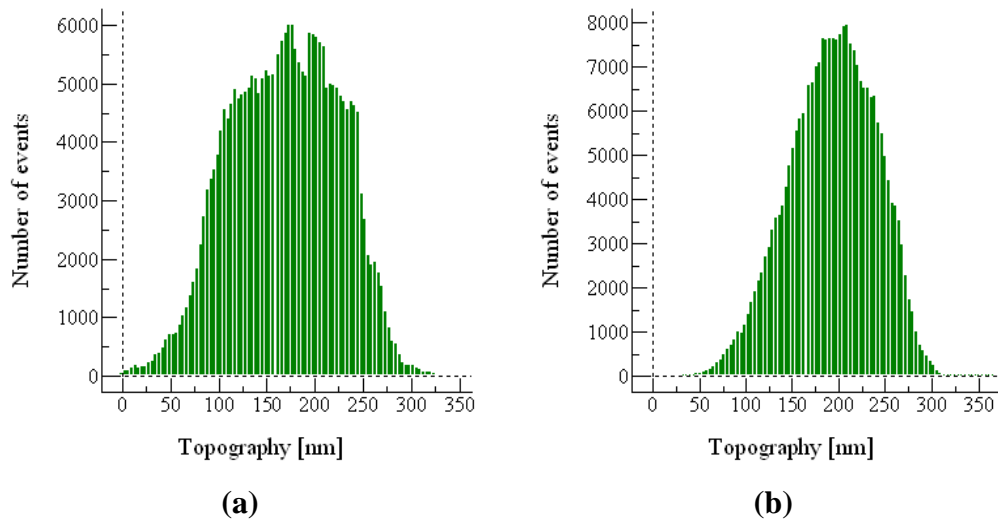


(a)

(b)

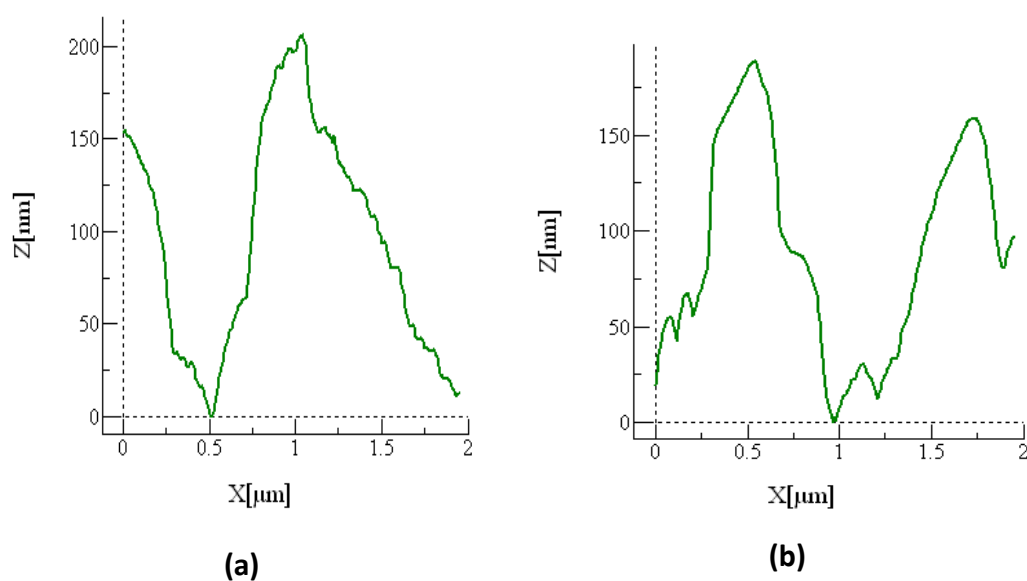
**Figure (3.17):** AFM images for a) naked rutile titanium dioxide thin film, b) rutile titanium dioxide thin film sensitized with curcumin.

Figure (3.18) shows the root mean square (RMS) roughness values obtained from average surface analysis for rutile titanium dioxide thin films. Rutile  $\text{TiO}_2$  thin films sensitized with curcumin exhibited RMS roughness of a bout  $\sim 200$  nm, while naked rutile  $\text{TiO}_2$  thin films exhibited RMS roughness of a bout  $\sim 170$  nm. This indicates that the grains showed nearly more coalescence in curcumine sensitized thin films than naked  $\text{TiO}_2$  thin films.



**Figure (3.18):** Average surface roughness analysis for a) naked rutile titanium dioxide thin film b) rutile titanium dioxide thin film sensitized with curcumin.

The surface depth profiling for the naked and curcumin sensitized rutile titanium dioxide thin films is shown in Figure (3.19). Holes and terraces with random distribution were found in both films but titanium dioxide films sensitized with curcumin showed higher cluster compactness.



**Figure (3.19):** Surface depth profiling for a) rutile titanium dioxide thin film b) rutile titanium dioxide thin film sensitized with curcumin.

The AFM results finally indicate that the rutile  $\text{TiO}_2$  films (both naked and sensitized) well adhered onto the FTO/ glass surface.

### 3.2. PEC Results:

The PEC characteristics for the prepared solar cells were measured at room temperature. Photo and dark J-V plots were measured by plotting current density ( $J = I / \text{area}$ ) vs. voltage (V). The stability of the solar cell was also measured and the results are presented.

### **3.2.1. Photo and dark J-V plots:**

Different parameters were applied to enhance the solar cells efficiencies as follows:

#### **3.2.1.1 Effect of type of natural dye:**

As mentioned before two types of natural dye were used to sensitize the solar cell. Effect of type of dye on cell PEC characteristic was studied. Curcumin and anthocyanin were both reported before as natural sensitizers for DSSCs. In this work we investigated different parameters. Anthocyanin was used for comparison. The effect of changing the pH value of curcumin system was studied before. Acidic conditions gave better results. Some structural changes on curcumin dye occurred and increased its conversion efficiency. Naked anatase and rutile titanium dioxide thin film electrodes gave no results under PEC conditions. Figure (3.20) shows the photo J-V plot for the curcumine sensitized solar cell and the anthocyanin sensitized solar cell. In both cases, anatase titanium dioxide was used to prepare the thin film electrodes for the cell.

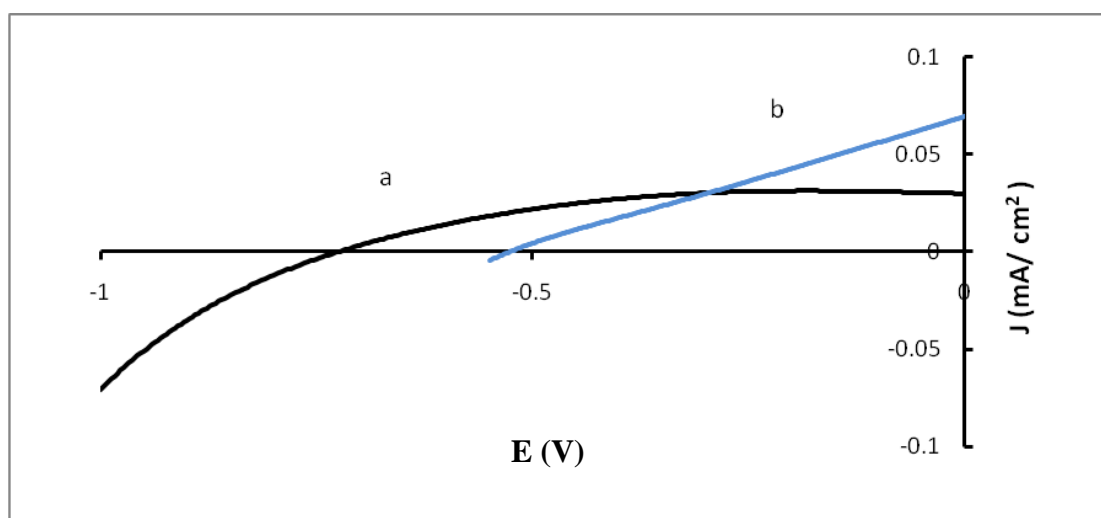


**Figure (3.20):** Photo J-V plot for a) anatase titanium dioxide thin film sensitized with curcumine b) anatase titanium dioxide thin film sensitized with anthocyanin extracted from roselle.

**Table (3.1): PEC characteristics for naked and curcumin sensitized anatase titanium dioxide thin films**

SAMPLE	$V_{oc}$	$J_{sc}$	$\square$	FF%
A	-0.75	0.03	0.22	59.5%
B	-0.53	0.07	0.13	21%

**A: curcumin sensitized anatase titanium dioxide thin film.**

**B: anthocyanin sensitized anatase titanium dioxide thin film.**

The Figure(3.20) indicates that curcumin sensitized solar cells gave better conversion efficiency and higher fill factor (Ratio between maximum observed efficiency divided by maximum possible efficiency) value as shown in Table (3.1). The Figure also shows that curcumin sensitized solar

cell gave a more negative  $V_{OC}$  (The applied potential at which current does not occur) value.

Figure (3.21) shows the photo J-V for rutile titanium dioxide solar cells sensitized with curcumin and anthocyanin. The Figure (3.21) indicates that curcumin also gave better results than anthocyanin sensitized solar cells.

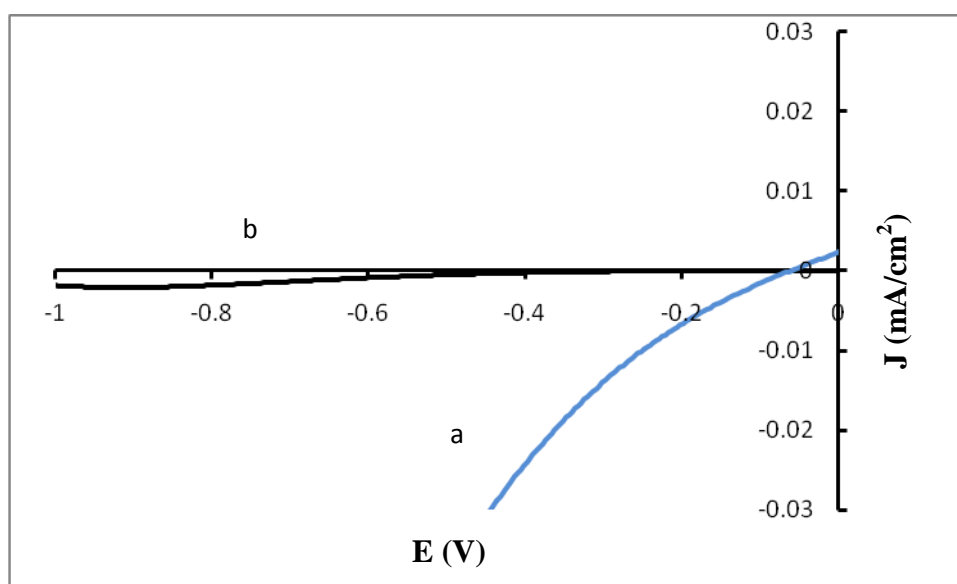


**Figure (3.21):** Photo J-V plot for a) rutile titanium dioxide thin film sensitized with curcumine b) rutile titanium dioxide thin film sensitized with anthocyanin extracted from roselle.

The UV-VIS absorption spectra indicate that curcumin absorbs at shorter wave length ( $\lambda$  412nm) which indicates a band gab value of about 3 eV anthocyanin absorbs at ( $\lambda$  545 nm ) with a band gab value of 2.3 eV. The difference in the band gab values increases the driving force of curcumin this explains the difference in values of  $V_{OC}$ . The molar absorptivity of curcumin is three times greater than the molar absorptivity of anthocyanin this explains the difference in values of  $J_{SC}$  (Short circuit current passing across a unit area of the semiconductor electrode). The schematic Figure

(3.22) explains the difference in the band gap values of curcumin and anthocyanin.

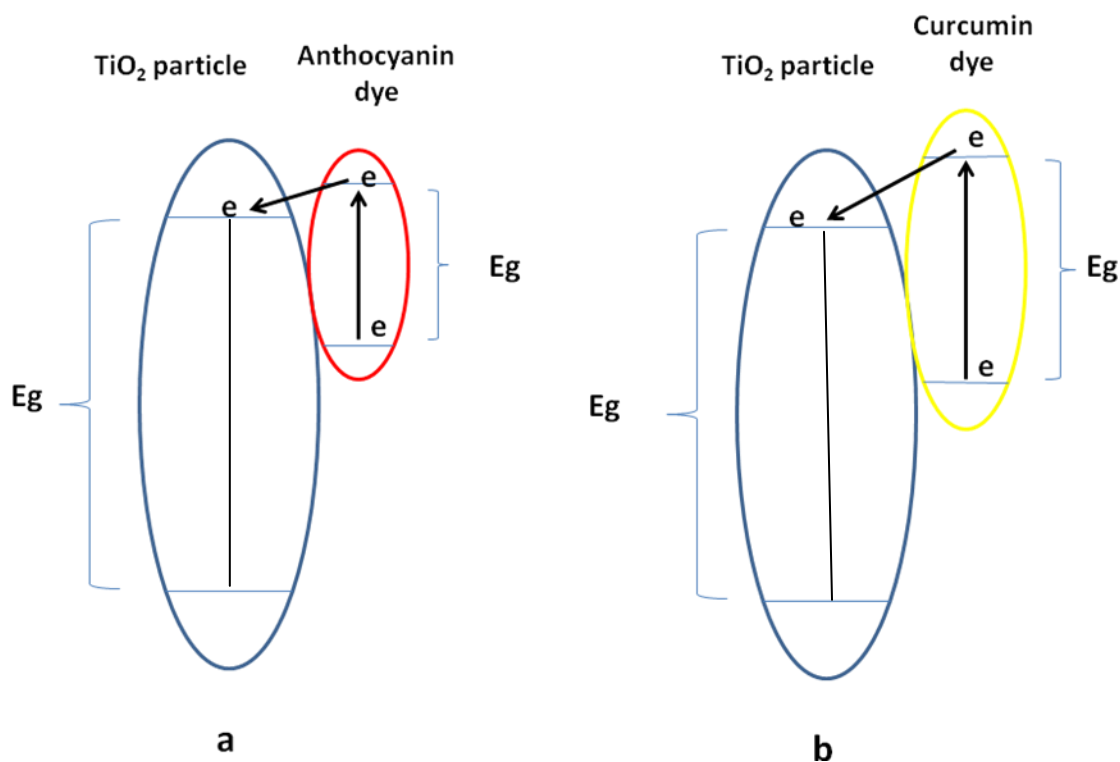


**Figure (3.22):** Schematic structure for a) anthocyanin dye particle b) curcumin dye particle.

From figures (3.20) and (3.21) it can be noticed that anatase titanium dioxide thin film electrodes gave a higher efficiency (when the solar cells were sensitized using curcumin or anthocyanin) than rutile counterparts.

Anthocyanin was extracted from three natural sources. The photo J-V plots for solar cells sensitized with three different kinds of dyes are presented in, Figure (3.23).

Figure (3.23) shows the photo J-V plots for anatase titanium dioxide solar cells sensitized with anthocyanin extracted from roselle, red cabbage and

beets. The figure indicates that anthocyanin extracted from roselle gave a better conversion efficiency and higher  $V_{OC}$  value than red cabbage. Beets anthocyanin sensitized solar cells gave no results. Table (3.2) summarizes the results.

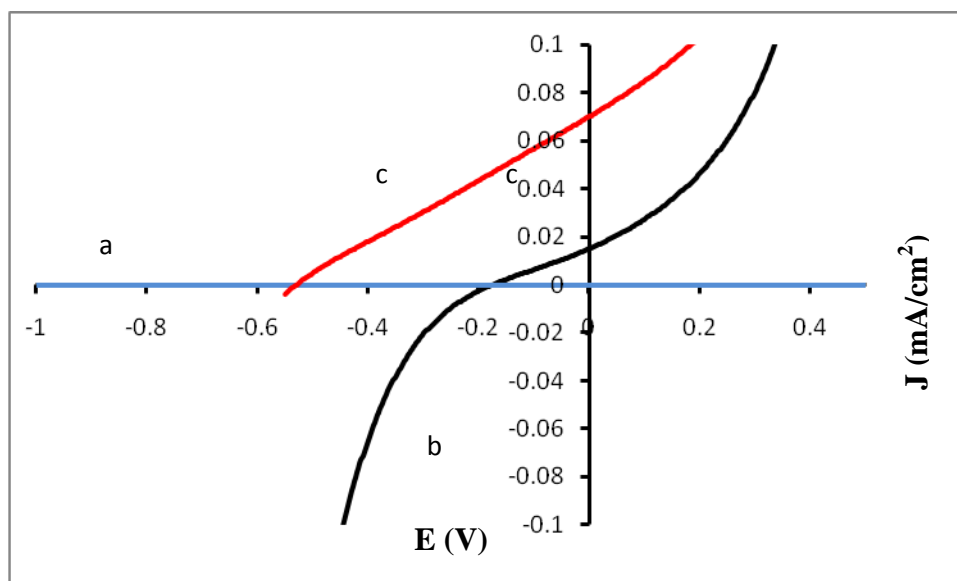


**Figure (3.23):** Photo J-V plot for a) anatase titanium dioxide thin film sensitized with anthocyanin extracted from beets b) anatase titanium dioxide thin film sensitized with anthocyanin extracted from red cabbage c) anatase titanium dioxide thin film sensitized with anthocyanin extracted from roselle.



**Table (3.2): PEC characteristics for anthocyanin sensitized anatase titanium dioxide thin films**

SAMPLE	$V_{oc}$	$J_{sc}$	$\square$	FF%
C	-0.53	0.07	0.13	21%
B	-0.2	0.019	0.02	37.6%

**C:** anatase titanium dioxide thin film sensitized with anthocyanin extracted from roselle.

**B:** anatase titanium dioxide thin film sensitized with anthocyanin extracted from red cabbage.

### 3.2.1.2 Effect of electrolyte:

The electrolyte used in DSSCs should affect ionic conductivity with better charge transfer. There are different kinds of aqueous and organic solvent electrolytes that can be used in DSSCs[22]. In our research three different types of aqueous electrolytes were used. Figure (3.24) shows the photo J-V plots for anatase titanium dioxide thin films sensitized with curcumine using iodine electrolyte, iron electrolyte and sulfur electrolyte. Iodine electrolyte gave the best results. The conversion efficiencies are shown in Table (3.3). Films measured using iron electrolyte didn't give any result.

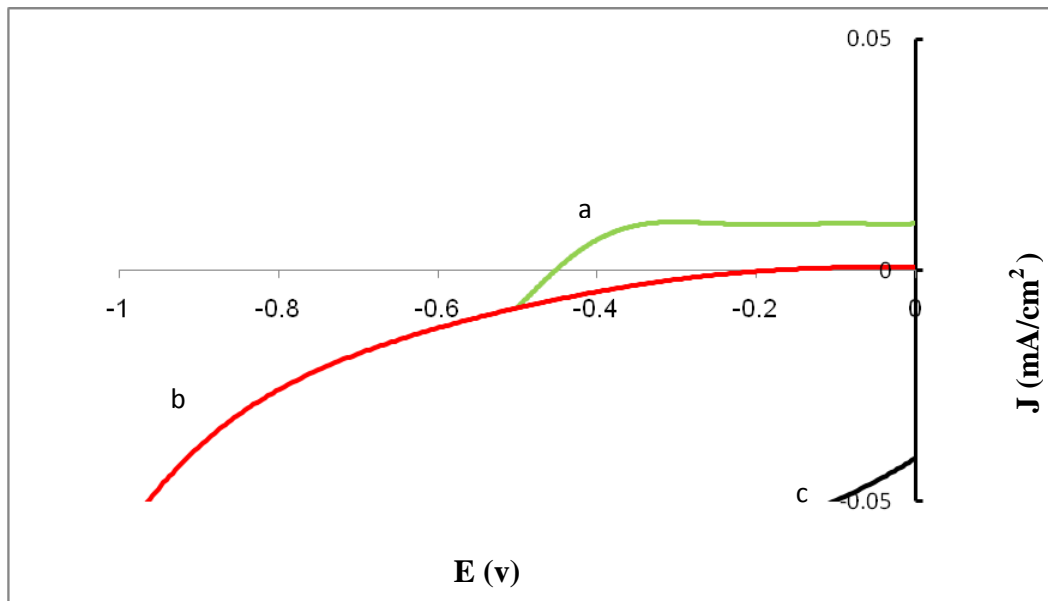


**Figure (3.24):** Photo J-V plot for a) anatase titanium dioxide thin film sensitized with curcumine using iodine electrolyte b) anatase titanium dioxide thin film sensitized with curcumine using sulfur electrolyte c) anatase titanium dioxide thin film sensitized with curcumine using iron electrolyte.

**Table (3.3):** effect of electrolyte type on PEC characteristics of anatase titanium dioxide thin films

SAMPLE	$V_{oc}$	$J_{sc}$	$\square$	FF%
A	-0.42	0.031	0.16	74.3%
B	-0.3	0.001	0.055	0%

**A:** anatase titanium dioxide thin film sensitized with curcumine using iodine electrolyte.

**B:** anatase titanium dioxide thin film sensitized with curcumine using sulfur electrolyte

Figure (3.25) shows the photo J-V plot for rutile titanium dioxide solar cells using all three types of aqueous lelectrolytes. Thin films measured

using iodine electrolyte gave the best results while using sulfur electrolyte gave no results. Table (3.4) shows the PEC characteristics.

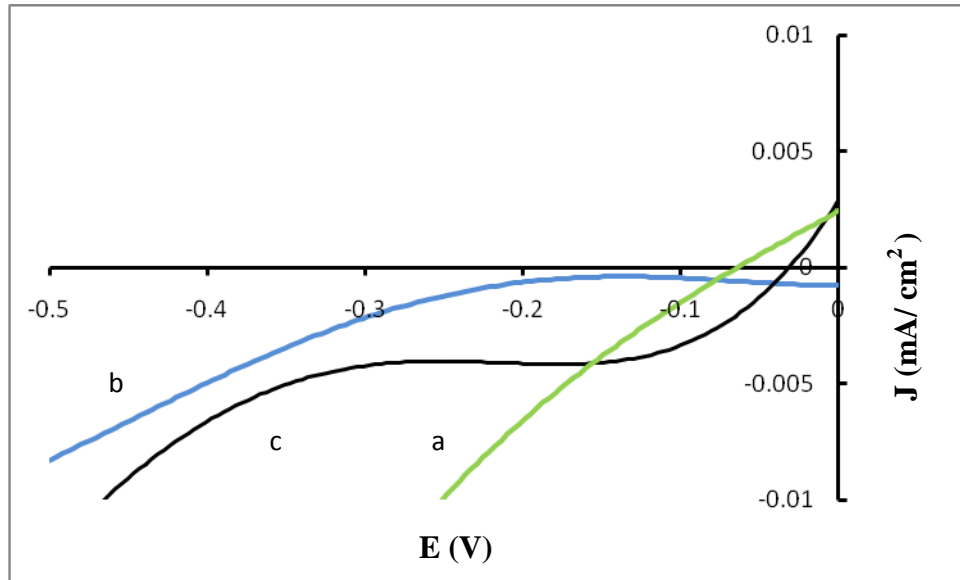


**Figure (3.25):** Photo J-V plot for rutile titanium dioxide thin film sensitized with curcumin using a) iodine electrolyte b) sulfur electrolyte c) iron electrolyte.

**Table (3.4):** Effect of electrolyte type on PEC characteristics of rutile titanium dioxide thin films

SAMPLE	$V_{oc}$	$J_{sc}$	$\square$	FF%
A	-0.06	0.022	0.03	22.72%
C	-0.04	0.03	0.01	0.83%

**A:** rutile titanium dioxide thin film sensitized with curcumin using iodine electrolyte.

**C:** rutile titanium dioxide thin film sensitized with curcumin using iron electrolyte

### 3.2.1.3 Effect of solution pH:

Both sulfur and iron electrolytes were used as prepared since changing their pH value may damage them. Iodine found to be acidic (pH = 3) as prepared, its pH was increased to reach 11. Figure (3.26) shows the photo J-V plots for anatase titanium dioxide thin films using iodine electrolyte after controlling its pH. Thin films using basic (pH= 11) iodine electrolyte gave better results with 0.22 conversion efficiency than films used in acidic iodine electrolyte with 0.16 conversion efficiency. At higher pH value, it can be guaranteed that all  $I^-$  ions remain in their free ionic ( $I^-$ ) form. In acidic medium, parts of  $I^-$  may be converted into HI molecular form.

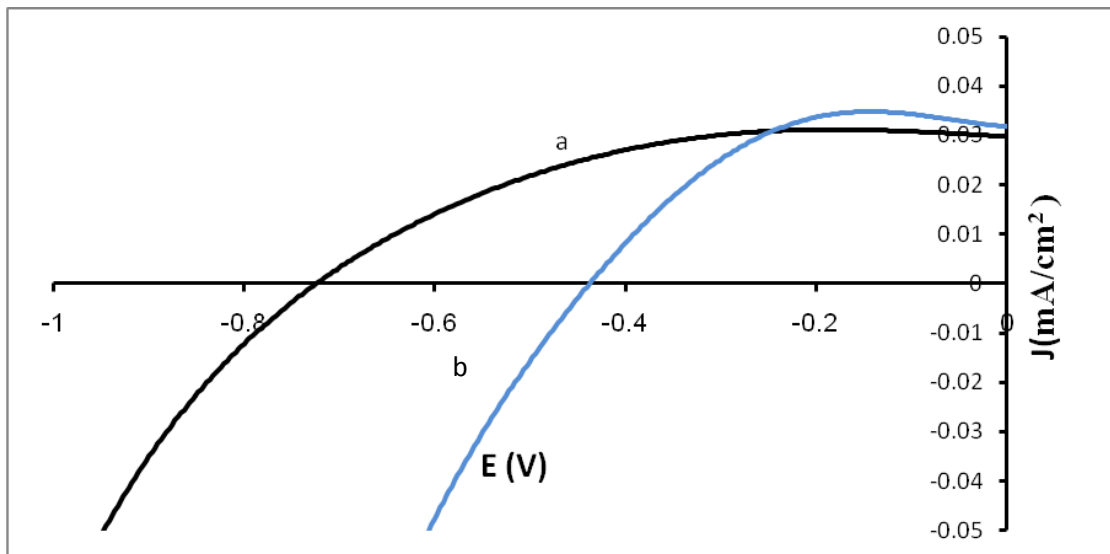


**Figure (3.26):** Photo J-V plot for a) anatase titanium dioxide thin film sensitized with curcumin using basic iodine electrolyte b) anatase titanium dioxide thin film sensitized with curcumin using acidic iodine electrolyte.

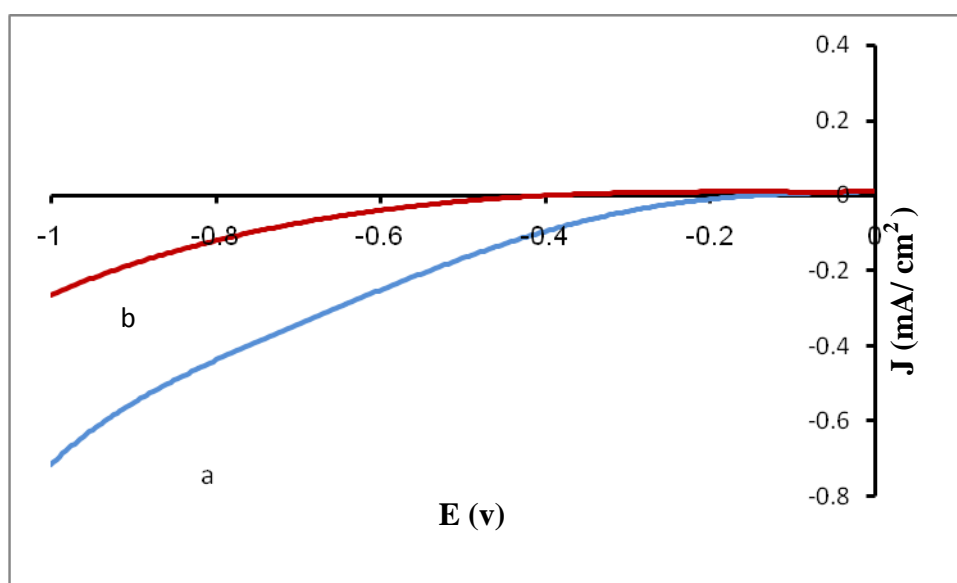
**Table (3.5): Effect of pH value of electrolyte on PEC characteristics of anatase titanium dioxide thin films**

SAMPLE	$V_{oc}$	$J_{sc}$	$\square$	FF%
A	-0.75	0.030	0.22	59.5%
B	-0.42	0.031	0.16	74.3%

**A:** anatase titanium dioxide thin film sensitized with curcumine using basic iodine electrolyte.

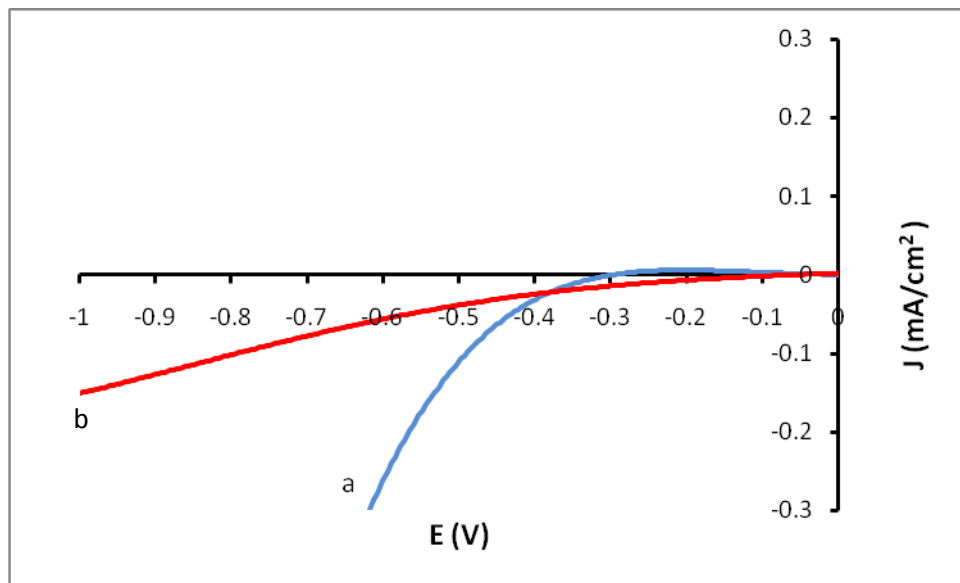
**B:** anatase titanium dioxide thin film sensitized with curcumine using acidic iodine electrolyte.

Figure (3.27) shows the dark J-V plot (Current that occurs in the dark with applied potential when the bands are falt) for anatase titanium dioxide thin films. Changing the pH value for the iodine electrolyte didn't enhance the dark currents.



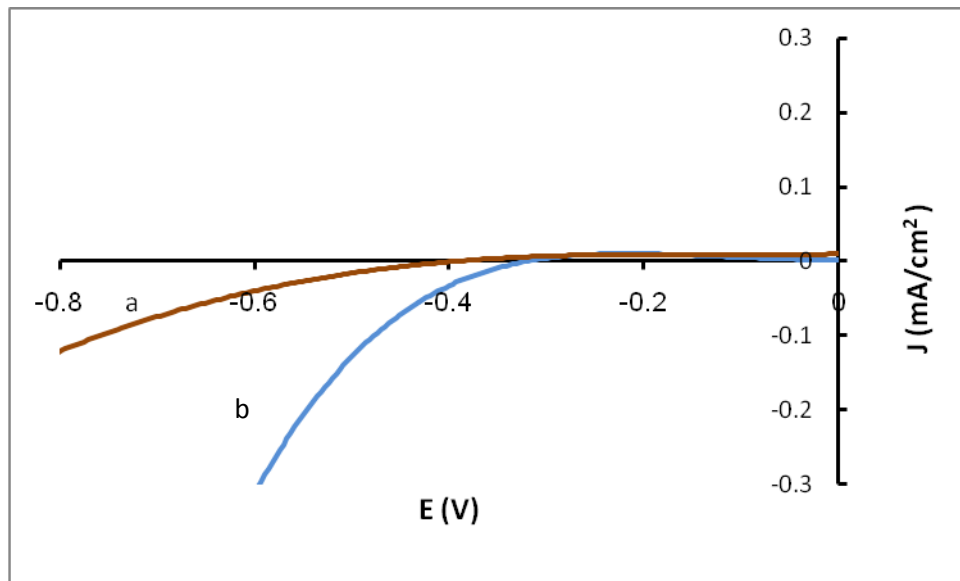
**Figure (3.27) :** Dark J-V plot for a) anatase titanium dioxide thin film sensitized with curcumine using acidic iodine electrolyte b) anatase titanium dioxide thin film sensitized with curcumine using basic iodine electrolyte.

Figure (3.28) shows the photo J-V plots for rutile titanium dioxide thin films sensitized with curcumine measured using iodine electrolyte with different pH values. Thin film electrodes measured with basic iodine electrolyte showed better results than films measured with acidic iodine electrolyte. But in both cases rutile  $\text{TiO}_2$  didn't give good results.



**Figure (3.28):** Photo J-V plot for rutile titanium dioxide thin film sensitized with curcumine using a) basic iodine electrolyte b) acidic iodine electrolyte.

Figure (3.29) shows dark J-V plots. No enhancement was observed on the dark current in both cases. The positive current values may be due to current leakage during the experiment.



**Figure (3.29):** Dark J-V plot for rutile titanium dioxide thin film sensitized with curcumin using a) basic iodine electrolyte b) acidic iodine electrolyte.

#### **3.2.1.4 Effect of thickness of titanium dioxide layer:**

Photo J-V plots were obtained for anatase titanium dioxide thin films (sensitized with curcumin) with different thickness, as shown in Figure (3.30). Titanium dioxide thin film with 150  $\mu\text{m}$  thickness gave better results than films with 130  $\mu\text{m}$  thickness. The 130  $\mu\text{m}$  film may not be thick enough so the light passes through the cell unaffected, increasing the film thickness above 150  $\mu\text{m}$  causes cracks in the solid thin film prepared by Dr. Blade technique. The conversion efficiencies are shown in Table (3.6)

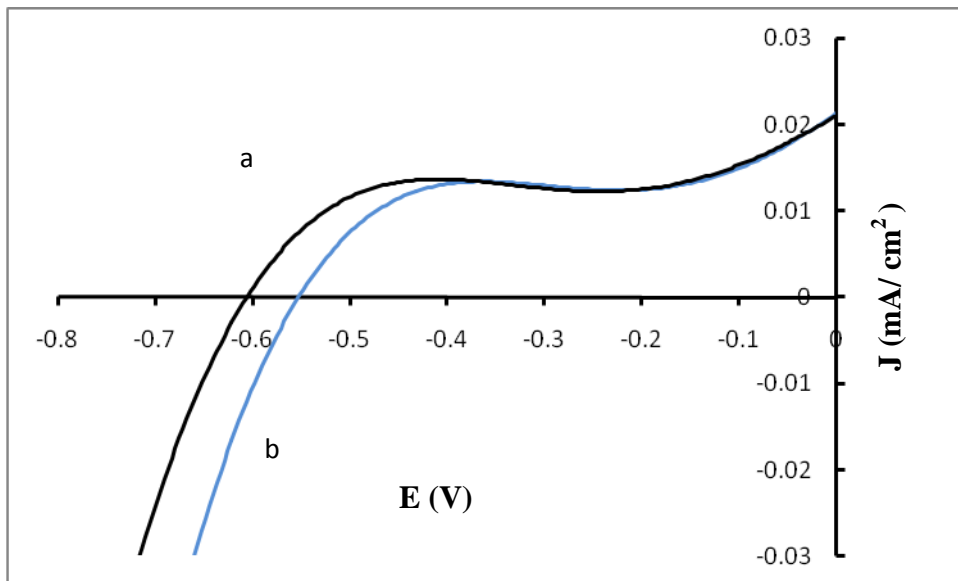


**Figure (3.30):** Photo J-V plot for a) Anatase titanium dioxide thin film with a 150  $\mu\text{m}$  thickness b) anatase titanium dioxide thin film with a 130  $\mu\text{m}$  thickness.

**Table (3.6):** Effect of layer thickness on PEC characteristics of anatase titanium dioxide thin films

SAMPLE	$V_{oc}$	$J_{sc}$	$\square$	FF%
A	-0.61	0.021	0.18	79.4%
B	-0.55	0.021	0.16	82.2%

**A:** anatase titanium dioxide thin film with a 150  $\mu\text{m}$  thickness.

**B:** anatase titanium dioxide thin film with a 130  $\mu\text{m}$  thickness.



Rutile titanium dioxide thin films were prepared with different thickness and photo J-V plots were obtained. Figure (3.31) shows that thin films with 150  $\mu\text{m}$  thickness shows better results than films with 130  $\mu\text{m}$  thickness.

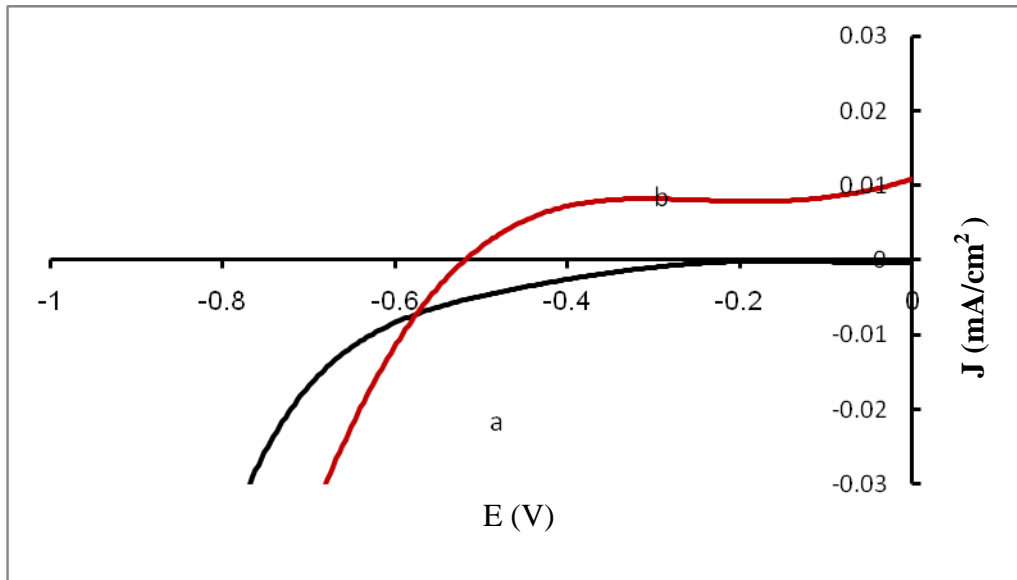


**Figure (3.31):** Photo J-V plot for a) rutile titanium dioxide thin film with a 130  $\mu\text{m}$  thickness b) rutile titanium dioxide thin film with a 150  $\mu\text{m}$  thickness.

**Table (3.7):** Effect of layer thickness on PEC characteristics of rutile titanium dioxide thin films

SAMPLE	$V_{oc}$	$J_{sc}$	$\square$	FF%
A	0	0	0	0%
B	-0.55	0.011	0.08	80.99%

**A:** rutile titanium dioxide thin film with a 130  $\mu\text{m}$  thickness.

**B:** rutile titanium dioxide thin film with a 150  $\mu\text{m}$  thickness.

### 3.2.1.5 Effect of titanium dioxide crystal type:

Anatase and rutile forms of titanium dioxide were reported to have structural and electronic differences. Here we are investigating the effect of titanium dioxide types, used to prepare the thin film electrode, on the curcumin sensitized solar cell efficiency. Figure (3.32) shows the photo J-V plot for anatase titanium dioxide thin film sensitized with curcumin and rutile titanium dioxide thin film sensitized with curcumin. The Figure (3.32) indicates that anatase titanium dioxide thin films gave better results with higher conversion efficiency. This could be attributed to the structural properties of anatase which increase the dye adsorption on the surface and facilitates electron transport.

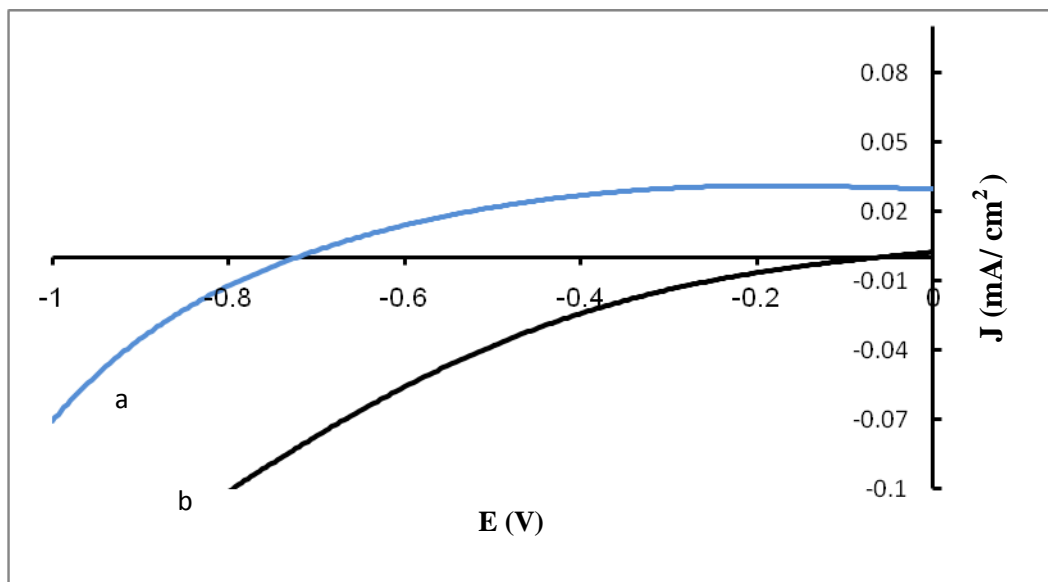


**Figure (3.32):** Photo J-V plot for a) anatase titanium dioxide thin film sensitized with curcumin b) rutile titanium dioxide thin film sensitized with curcumin.

**Table (3.8): Effect of type of titanium dioxide on PEC characteristics of thin films**

SAMPLE	$V_{oc}$	$J_{sc}$	$\square$	FF%
A	-0.75	0.03	0.22	59.5%
B	-0.06	0.022	0.03	22.72%

**A: anatase titanium dioxide thin film.**

**B: rutile titanium dioxide thin film.**

Figure (3.33) shows the dark J-V plot for anatase titanium dioxide thin film and rutile titanium dioxide thin film both sensitized with curcumin. Both films showed dark currents with leakage current flows.

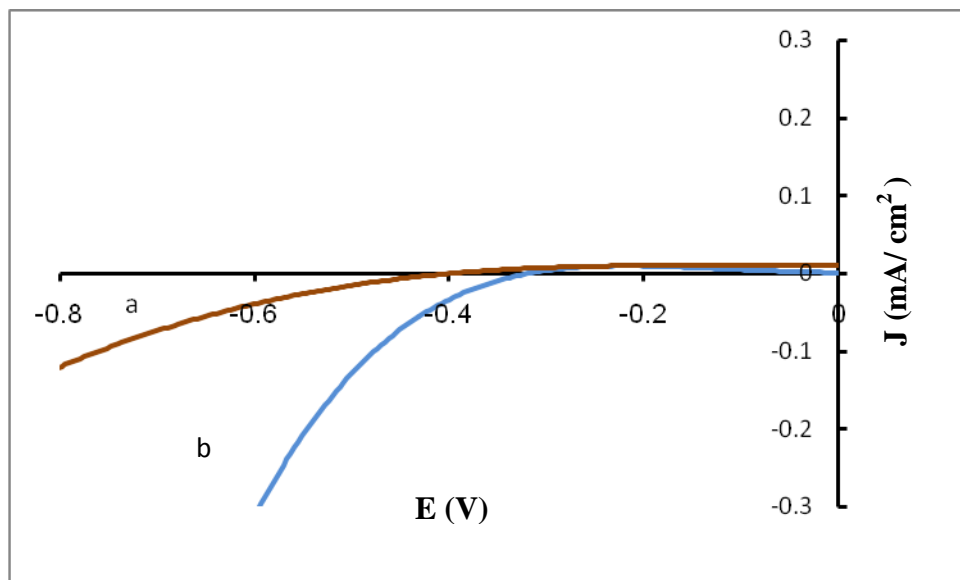


**Figure (3.33):** Dark J-V plot for a) anatase titanium dioxide thin film sensitized with curcumin  
b) rutile titanium dioxide thin film sensitized with curcumin.

### 3.3 Stability measurement:

The solar cell stability under PEC conditions was investigated for the anatase titanium dioxide thin film sensitized with curcumin. The  $J_{SC}$  vs. time was measured Figure (3.34). The measurement was conducted using basic iodine electrolyte at room temperature. The Figure indicates that the anatase titanium dioxide solid thin film was stable for at least 150 min.

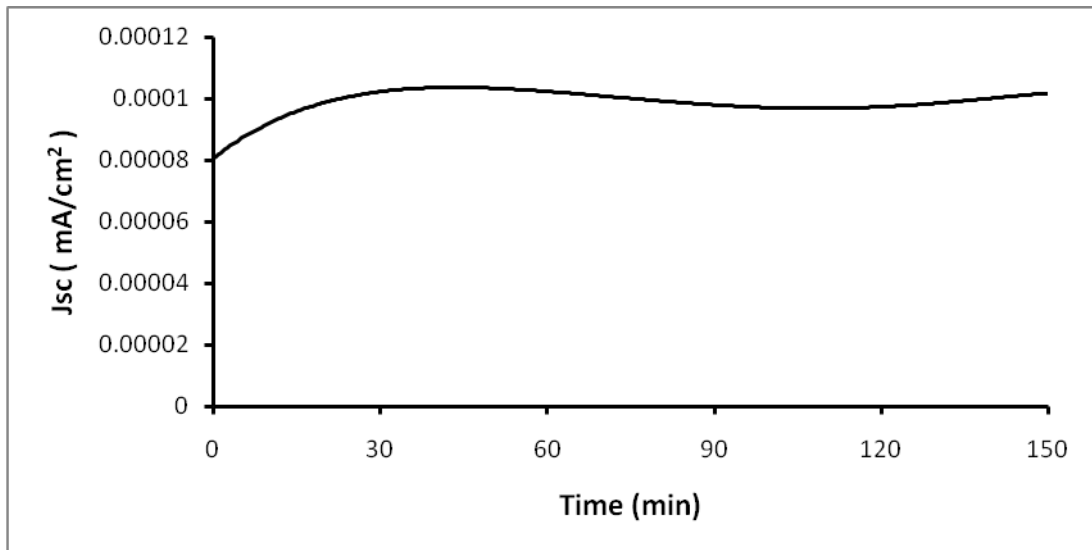


**Figure (3.34):** Short circuit current density vs. time measured for anatase titanium dioxide thin film electrode sensitized with curcumine.

## Conclusion

In this study, several parameters were investigated to enhance the work efficiency of the prepared dye sensitized solar cell. Dr. Blade technique was used to prepare the titanium dioxide electrodes. From the results we can draw these conclusions:

1- Anatase titanium dioxide thin films gave better conversion efficiencies than rutile titanium dioxide thin films in all types of solar cells.

2- Better work efficiency was obtained using curcumin as photosensitizer for the prepared dye sensitized solar cells.

3- The solar cell work efficiency was affected by the type of redox couple. Iodine electrolyte gave better results than sulfur and iron electrolytes in the PEC measurements.

4- Changing the pH value of the used redox couple strongly affected the efficiency of the solar cell. Higher conversion efficiencies were obtained using basic iodine solutions.

5- Changing the pH value for both iron and iodine electrolytes destroys them.

6- Anatase and rutile titanium dioxide thin films with 130  $\mu\text{m}$  thickness gave better conversion efficiencies.

## **Recommendations for Future Work**

1- Investigate the effect of changing the pH value and using other redox couples such as Co electrolyte on the curcumin sensitized solar cell.

2- Further study of the photoluminescence and IR characteristics for the prepared titanium dioxide thin films sensitized with curcumin.

3- Study the SEM and TEM properties of the prepared titanium dioxide thin films sensitized with curcumin.

4- Prepare a thin film using a mixture of both types of titanium dioxide powders (anatase and rutile).

5- Study the effect of temperature of the curcumin dye solution on the solar cell efficiency.

6- Apply the recommended optimum conditions on the curcumin dye sensitized solar cell using ZnO semiconductors.

## References

- [1] M. Zeman, **Introduction to Photovoltaic Solar Energy**, Solar Cells, collegemateriaal, (2003).
- [2] N. Panwar, S. Kaushik, S. Kothari, **Role of renewable energy sources in environmental protection: a review**, **Renewable and Sustainable Energy Reviews**, 15 (2011) 1513-1524.
- [3] A.V. Herzog, T.E. Lipman, D.M. Kammen, **Renewable energy sources**, **Encyclopedia of Life Support Systems (EOLSS)**. Forerunner Volume-‘Perspectives and Overview of Life Support Systems and Sustainable Development, (2001).
- [4] T.B. Johansson, L. Burnham, **Renewable energy: sources for fuels and electricity**, Island Press, 1993.
- [5] S. Dimitrijević, **Principles of semiconductor devices**, Oxford university press Oxfordm UK, 2006.
- [6] P. Würfel, U. Würfel, **Physics of Solar Cells: From Basic Principles to Advanced Concepts**, John Wiley & Sons, 2009.
- [7] R. de Boer, R. de Boer, P. Bach, P. Alderliesten, E.E. Efficiency, **Technologies and prospects for photochemical conversion and storage of solar energy**, (2001).
- [8] R. Vijayalakshmi, V. Rajendran, **Synthesis and characterization of nano-TiO<sub>2</sub> via different methods**, **Archives of Applied Science Research**, 4 (2012).



- [9] M. Grätzel, **Dye-sensitized solar cells**, *Journal of Photochemistry and Photobiology C: Photochemistry Reviews*, 4 (2003) 145-153.
- [10] K. Kalyanasundaram, **Dye-sensitized solar cells**, EPFL press, 2010.
- [11] B. O'regan, M. Grfitzeli, **A low-cost, high-efficiency solar cell based on dye-sensitized**, *nature*, 353 (1991) 737-740.
- [12] A.S. Polo, M.K. Itokazu, N.Y. Murakami Iha, **Metal complex sensitizers in dye-sensitized solar cells**, *Coordination Chemistry Reviews*, 248 (2004) 1343-1361.
- [13] K.-I. Jang, E. Hong, J.H. Kim, **Effect of an electrodeposited TiO<sub>2</sub> blocking layer on efficiency improvement of dye-sensitized solar cell**, *Korean Journal of Chemical Engineering*, 29 (2012) 356-361.
- [14] K. Kalyanasundaram, N. Vlachopoulos, V. Krishnan, A. Monnier, M. Grätzel, **Sensitization of titanium dioxide in the visible light region using zinc porphyrins**, *Journal of Physical Chemistry*, 91 (1987) 2342-2347.
- [15] O. Enea, J. Moser, M. Grätzel, **Achievement of incident photon to electric current conversion yields exceeding 80% in the spectral sensitization of titanium dioxide by coumarin**, *Journal of electroanalytical chemistry and interfacial electrochemistry*, 259 (1989) 59-65.

- [16] Y. Chiba, A. Islam, Y. Watanabe, R. Komiya, N. Koide, L. Han, **Dye-sensitized solar cells with conversion efficiency of 11.1%**, *Japanese Journal of Applied Physics*, 45 (2006) L638.
- [17] P. Wang, S.M. Zakeeruddin, J.E. Moser, M.K. Nazeeruddin, T. Sekiguchi, M. Grätzel, **A stable quasi-solid-state dye-sensitized solar cell with an amphiphilic ruthenium sensitizer and polymer gel electrolyte**, *Nature materials*, 2 (2003) 402-407.
- [18] H. Zhou, L. Wu, Y. Gao, T. Ma, **Dye-sensitized solar cells using 20 natural dyes as sensitizers**, *Journal of Photochemistry and Photobiology A: Chemistry*, 219 (2011) 188-194.
- [19] K. Hara, H. Arakawa, **Dye-sensitized solar cells**, *Handbook of Photovoltaic Science and Engineering*, 6634696 (2003).
- [20] H.-J. Kim, D.-J. Kim, S. Karthick, K. Hemalatha, C.J. Raj, **Curcumin Dye Extracted from Curcuma longa L. Used as Sensitizers for Efficient Dye-Sensitized Solar Cells**, *International Journal of Electrochemical Science*, 8 (2013).
- [21] P.R. Somani, S.P. Somani, M. Umeno, A. Sato, **Concept and demonstration of all organic Gratzel solar cell (dye sensitized solar cell)**, *Applied physics letters*, 89 (2006) 83501.
- [22] D. Wei, **Dye sensitized solar cells**, *International journal of molecular sciences*, 11 (2010) 1103-1113.

- [23] S.A. Al-Bat'hi, I. Alaei, I. Sopyan, **Natural Photosensitizers for Dye Sensitized Solar Cells**, International Journal of Renewable Energy Research (IJRER), 3 (2013) 138-143.
- [24] S. Suhaimi, M.M. Shahimin, I.S. Mohamad, M.N. Norizan, **Comparative Study of Natural Anthocyanins Compound as Photovoltaic Sensitizer**, (2013).
- [25] C.F. Chignell, P. Bilskj, K.J. Reszka, A.G. Motten, R.H. Sik, T.A. Dahl, **Spectral and photochemical properties of curcumin**, *Photochemistry and photobiology*, 59 (1994) 295-302.
- [26] B.B. Aggarwal, C. Sundaram, N. Malani, H. Ichikawa, **Curcumin: the Indian solid gold, in: The molecular targets and therapeutic uses of curcumin in health and disease**, Springer, 2007, pp. 1-75.
- [27] P. Anand, A.B. Kunnumakkara, R.A. Newman, B.B. Aggarwal, **Bioavailability of curcumin: problems and promises**, *Molecular pharmaceutics*, 4 (2007) 807-818.
- [28] Z.-S. Wang, K. Hara, Y. Dan-oh, C. Kasada, A. Shinpo, S. Suga, H. Arakawa, H. Sugihara, **Photophysical and (photo) electrochemical properties of a coumarin dye**, *The Journal of Physical Chemistry B*, 109 (2005) 3907-3914.
- [29] Z.-S. Wang, Y. Cui, Y. Dan-oh, C. Kasada, A. Shinpo, K. Hara, **Thiophene-functionalized coumarin dye for efficient dye-sensitized**

**solar cells: electron lifetime improved by coadsorption of deoxycholic acid**, *The Journal of Physical Chemistry C*, 111 (2007) 7224-7230.

[30] M.J. Eiro, M. Heinonen, **Anthocyanin color behavior and stability during storage: effect of intermolecular copigmentation**, *Journal of agricultural and food chemistry*, 50 (2002) 7461-7466.

[31] R. Brouillard, **The expression of anthocyanin colour in plants**, *Phytochemistry*, 22 (1983) 1311-1323.

[32] T. Fossen, L. Cabrita, O.M. Andersen, **Colour and stability of pure anthocyanins influenced by pH including the alkaline region**, *Food Chemistry*, 63 (1998) 435-440.

[33] R. Brouillard, **Chemical structure of anthocyanins**, **Academic Press**: New York, 1982.

[34] J.-M. Kong, L.-S. Chia, N.-K. Goh, T.-F. Chia, R. Brouillard, **Analysis and biological activities of anthocyanins**, *Phytochemistry*, 64 (2003) 923-933.

[35] Y. Li, F. Piret, T. Léonard, B.-L. Su, **Rutile TiO<sub>2</sub> inverse opal with photonic bandgap in the UV-visible range**, *Journal of colloid and interface science*, 348 (2010) 43-48.

[36] F.M. Hossain, L. Sheppard, J. Nowotny, G.E. Murch, **Optical properties of anatase and rutile titanium dioxide: Ab initio calculations**

for pure and anion-doped material, *Journal of Physics and Chemistry of Solids*, 69 (2008) 1820-1828.

[37] M. Quintana, T. Edvinsson, A. Hagfeldt, G. Boschloo, **Comparison of dye-sensitized ZnO and TiO<sub>2</sub> solar cells: studies of charge transport and carrier lifetime**, *The Journal of Physical Chemistry C*, 111 (2007) 1035-1041.

[38] W. Macyk, K. Szaciłowski, G. Stochel, M. Buchalska, J. Kunczewicz, P. Łabuz, **Titanium (IV) complexes as direct TiO<sub>2</sub> photosensitizers**, *Coordination Chemistry Reviews*, 254 (2010) 2687-2701.

[39] H. Yang, S. Zhu, N. Pan, **Studying the mechanisms of titanium dioxide as ultraviolet-blocking additive for films and fabrics by an improved scheme**, *Journal of Applied Polymer Science*, 92 (2004) 3201-3210.

[40] H.R. Beratan, S.R. Summerfelt, **Semiconductor structures using high-dielectric-constant materials and an adhesion layer**, in, *Google Patents*, 1997.

[41] A.A. Gribb, J.F. Banfield, **Particle size effects on transformation kinetics and phase stability in nanocrystalline TiO<sub>2</sub>**, *American Mineralogist*, 82 (1997) 717-728.

[42] P. Kajitvichyanukul, J. Ananpattarachai, S. Pongpom, **Sol-gel preparation and properties study of TiO<sub>2</sub> thin film for photocatalytic**

**reduction of chromium (VI) in photocatalysis process**, Science and technology of advanced materials, 6 (2005) 352-358.

[43] J. Lyon, M. Rayan, M. Beerbom, R. Schlaf, **Electronic structure of the indium tin oxide/nanocrystalline anatase (TiO<sub>2</sub>)/ruthenium-dye interfaces in dye-sensitized solar cells**, *Journal of Applied Physics*, 104 (2008) 073714.

[44] D. Scaife, **Oxide semiconductors in photoelectrochemical conversion of solar energy**, *Solar Energy*, 25 (1980) 41-54.

[45] G. Schlichthörl, S. Huang, J. Sprague, A. Frank, **Band edge movement and recombination kinetics in dye-sensitized nanocrystalline TiO<sub>2</sub> solar cells: a study by intensity modulated photovoltage spectroscopy**, *The Journal of Physical Chemistry B*, 101 (1997) 8141-8155.

[46] N. Serpone, D. Lawless, R. Khairutdinov, **Size effects on the photophysical properties of colloidal anatase TiO<sub>2</sub> particles: size quantization versus direct transitions in this indirect semiconductor?**, *The journal of Physical Chemistry*, 99 (1995) 16646-16654.

[47] T. Wen, J. Gao, J. Shen, Z. Zhou, **Preparation and characterization of TiO<sub>2</sub> thin films by the sol-gel process**, *Journal of materials science*, 36 (2001) 5923-5926.

- [48] Z. Zhang, C.-C. Wang, R. Zakaria, J.Y. Ying, **Role of particle size in nanocrystalline TiO<sub>2</sub>-based photocatalysts**, *The Journal of Physical Chemistry B*, 102 (1998) 10871-10878.
- [49] K. Madhusudan Reddy, C. Gopal Reddy, S. Manorama, **Preparation, Characterization, and Spectral Studies on Nanocrystalline Anatase TiO<sub>2</sub>**, *Journal of Solid State Chemistry*, 158 (2001) 180-186.
- [50] S.K. Salih, **Modification of The Properties of Cadmium Selenid Thin Films In Photovoltaic Solar Cells**, in, National University, 2009.
- [51] D. Chen, M. Sivakumar, A.K. Ray, **Heterogeneous photocatalysis in environmental remediation**, *Developments in Chemical Engineering and Mineral Processing*, 8 (2000) 505-550.
- [52] n.m. abrams, **efficiency enhancement in dye sensitized solar cells through light manipulation**, master thesis, (2005).
- [53] J. Cacace, G. Mazza, **Optimization of extraction of anthocyanins from black currants with aqueous ethanol**, *Journal of Food Science*, 68 (2003) 240-248.
- [54] H. Pabon, **A synthesis of curcumin and related compounds**, *Recueil des Travaux Chimiques des Pays-Bas*, 83 (1964) 379-386.

جامعة النجاح الوطنية

كلية الدراسات العليا

## انواع جديدة من الخلايا الضوئية المنشطة بالاصباغ الطبيعية

اعداد

ملاك صبيح احمد سيف

اشراف

أ.د. حكمت هلال

د. عاهد زيود

قدمت هذه الأطروحة استكمالاً لمتطلبات الحصول على درجة الماجستير في الكيمياء بكلية الدراسات العليا في جامعة النجاح الوطنية ، نابلس - فلسطين.

2014



## أنواع جديدة من خلايا شمسية منشطة بالأصبغ الطبيعية

إعداد

ملاك صبيح احمد سيف

إشراف

أ.د. حكمت هلال

د. عاهد زيود

المخلص

تم إنتاج أنواع جديدة من الخلايا الشمسية المنشطة بالأصبغ الطبيعية (DSSCs)، وجرى التحقق من معايير مختلفة لتعزيز كفاءتها. تم استخدام نوعين من مساحيق ثاني أكسيد التيتانيوم ( $TiO_2$ ) لتحضير الأفلام الرقيقة للخلية.

استخدمت تقنية (Dr. Blade) في تحضير الأفلام الرقيقة لكلا النوعين من ثاني أكسيد التيتانيوم (Anatase, rutile) وقد اثبت (anatase) كفاءة عالية في تحويل الطاقة الشمسية إلى طاقة كهربائية فضلاً عن (rutile). استخدم نوعين من الأصباغ الطبيعية لتنشيط الخلايا الشمسية الكركم، والأنثوسيانين الذي استخرج من ثلاثة مصادر طبيعية: الملفوف الأحمر واللفت والكركديه. أكدت الدراسة على أن الخلايا الشمسية المنشطة بالكركم أعطت نتائج أفضل من نظائرها الأخرى.

تم استخدام ثلاثة أنواع مختلفة من أزواج التأكسد والإختزال: اليود، الحديد، والكبريت وقد وجد أن الخلايا التي تم قياسها باستخدام اليود كزوج تأكسد وإختزال أعطت أفضل النتائج في تحويل الضوء إلى كهرباء سواء في كلا الخلايا المنشطة بالكركم أو الأنثوسيانين على حد سواء. أثبتت الدراسة أن استخدام اليود كزوج تأكسد وإختزال في بيئة قاعدية يعطي نتائج أفضل من استخدامه في بيئة حامضية.

ج

تم انتاج أفلام من ثاني أكسيد التيتانيوم بسمكين مختلفين ( 130,150µm ) وقد وجد أن استخدام أفلام بسماكة 150 µm في بناء الخلايا الشمسية يعطي نتائج أفضل لكلا النوعين من ثاني اكسيد التيتانيوم (Anatase, Rutile).

